Optical Spectroscopy of Materials for Mid-Wave Infrared Detector Applications

Stefan Zollner,
Carlos A. Armenta, Sonam Yadav, Yoshitha Hettige, (Ph.D. students)
Jaden R. Love, Haley B. Woolf, Atlantis K. Moses, (MS students)
Danissa P. Ortega (UG student)

Department of Physics
New Mexico State University, Las Cruces, NM, 88007

Supported by:
AFOSR (FA9550-20-1-0135, FA9550-24-1-0061, SFFP)
AFRL/RVSU (FA9453-23-2-0001)
ARO (W911NF-22-2-0130)
NSF (DMR-2235447, DMR-2423992)
SCALE-RH (W52P1J-22-9-3009), J. A. Woollam Foundation

NM STATE **BE BOLD.** Shape the Future.

Email: zollner@nmsu.edu
Web: http://femto.nmsu.edu

New Mexico State University, Las Cruces

Land grant institution, Carnegie R2 (soon to be R1)
Comprehensive: Arts and Sciences, Education, Business, Agriculture
Ph.D. programs in sciences, engineering, agriculture; Ag extension;
Chile Pepper Institute

12,700 students (11,000 UG, 1,700 GR), 1000 faculty

Minority-serving, Hispanic-serving (60% Hispanic/NA, 26% White)
Small-town setting (111,000)

Military-friendly institution (Army and Air Force ROTC programs)

Community engagement classification
(first-generation students, Pell grant recipients)

Physics: BS/BA, MS, PhD degrees. 67 UG and 39 GR students.
11 faculty (HE Nuclear and Materials Physics), **2.4 M$ research expenditures.**
ABET-accredited BS in Physics and BS in Engineering Physics

Problem statement

(1) Achieve a **quantitative** understanding of **photon absorption** and **emission** processes.

- Our **qualitative** understanding of excitonic absorption is 50-100 years old (Einstein coefficients),
- But **insufficient** for modeling of detectors and emitters.

(2) How are optical processes affected by **high carrier concentrations** (screening)?

- High carrier densities can be achieved with
  - In situ doping or
  - **ultrafast (femtosecond) lasers** or
  - **high temperatures** (narrow-gap or gapless semiconductors)
- **Application:** CMOS-integrated mid-infrared camera (thermal imaging with a phone).
- Future: How are optical processes affected by an electric field (pin diode or thin layer)?

Application:
Midwave Infrared Detectors
Germanium-Tin Alloys

Intensity of Optical Absorption by Excitons

R. J. Elliott
Phys. Rev. **108**, 1384 – Published 15 December 1957

Article | References | Citing Articles (1,780) | PDF | Export Citation

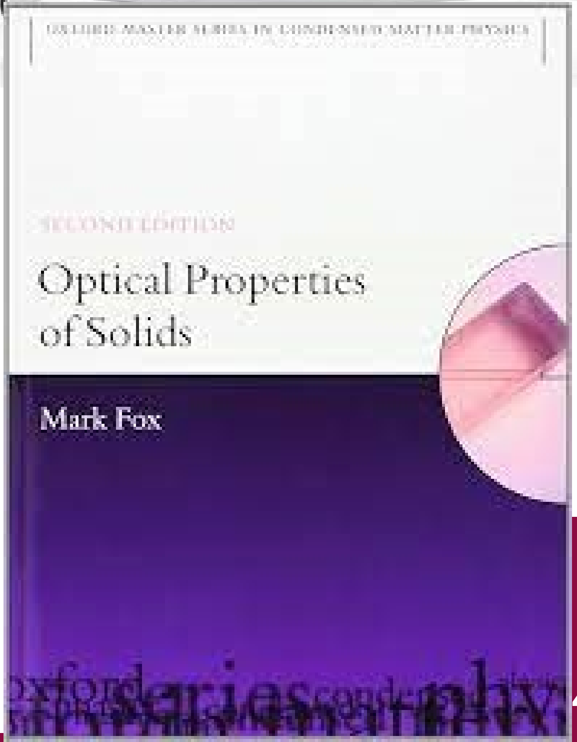

ABSTRACT

The intensity of optical absorption close to the edge in semiconductors is examined using band theory together with the effective-mass approximation for the excitons. Direct transitions which occur when the band extrema on either side of the forbidden gap are at the same **K**, give a line spectrum and a continuous absorption of characteristically different form and intensity, according as transitions between band states at the extrema are allowed or forbidden. If the extrema are at different **K** values, indirect transitions involving phonons occur, giving absorption proportional to $(\Delta E)^{\frac{1}{2}}$ for each exciton band, and to $(\Delta E)^2$ for the continuum. The experimental results on Cu_2O and Ge are in good qualitative agreement with direct forbidden and indirect transitions, respectively.

Received 9 April 1957

Ellipsometry at NMSU

diamond windows
closed-cycle He cooler

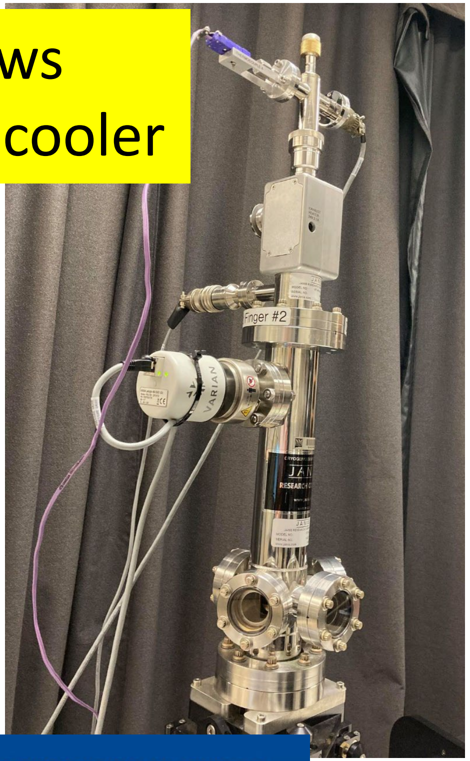

Ellipsometry on anything (inorganic, 3D)

- Metals, insulators, semiconductors
- Mid-IR to vacuum UV (150 nm to 40 μm)
- **10 to 800 K, ultrafast ellipsometry**

Ellipsometry tells us a lot about materials quality (not necessarily what we want to know).

[Optical critical points of thin-film $Ge_{1-y}Sn_y$ alloys: A comparative $Ge_{1-y}Sn_y$ / $Ge_{1-x}Si_x$ study] VR D'costa, CS Cook, AG Birdwell, CL Littler, M Canonico, S Zollner, ... Physical Review B—Condensed Matter and Materials Physics 73 (12), 125207	440	2006
Growth and strain compensation effects in the ternary $Si_{1-x-y}Ge_xC_y$ alloy system K Eberl, SS Iyer, S Zollner, JC Tsang, FK LeGoues Applied physics letters 60 (24), 3033-3035	397	1992
Ge–Sn semiconductors for band-gap and lattice engineering M Bauer, J Taraci, J Tolle, AVG Chizmeshya, S Zollner, DJ Smith, ... Applied physics letters 81 (16), 2992-2994	335	2002

http://femto.nmsu.edu

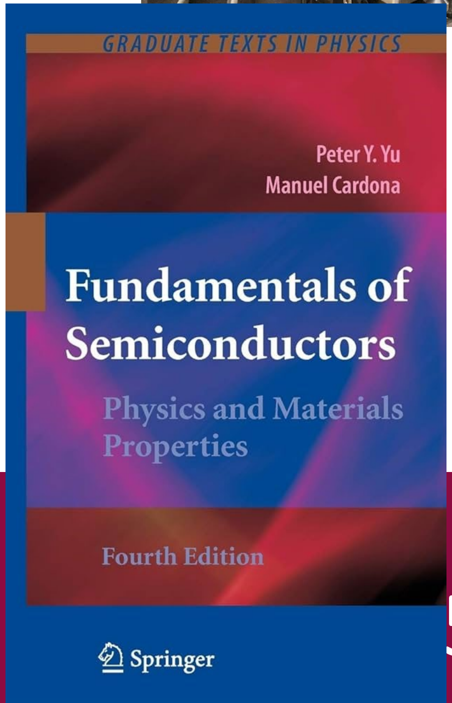

Optical Spectroscopy of Materials for Mid-Wave Infrared Detector Applications

1. **Pressure dependence** of low-temperature photoluminescence of germanium-tin alloys (AFRL/RVSU); Today: Temperature dependence of photoluminescence of bulk **GaSb**.
2. **Thermal oxidation** of **bulk Ge**, thick Ge on Si, and Ge-Sn alloys on Si (NSF, Arizona State); Include AFM surface roughness and structural characterization with high-resolution XRD.
3. **Nonparabolicity** of conduction band of InSb (SFFP, AFOSR)
4. Direct gap **infrared absorption of α-tin** with nonparabolic bands (SFFP, AFOSR)
5. Low-temperature ellipsometry measurements (0.03 to 6.5 eV) with a **recirculating helium cooler** (ARO).
6. **Direct gap absorption of α-tin** on InSb and CdTe: experiment and theory (NSF, UCSB)
7. Excitonic enhancement of the absorption near the E_1 gaps of Ge (AFOSR)
8. Transient dielectric function of germanium from **femtosecond pump-probe ellipsometry** (AFOSR)

Email: zollner@nmsu.edu
Web: http://femto.nmsu.edu

Temperature-dependent photoluminescence of GaSb

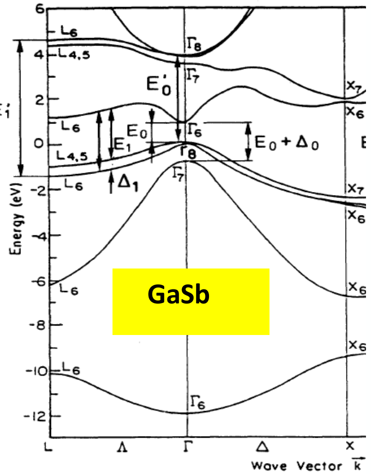

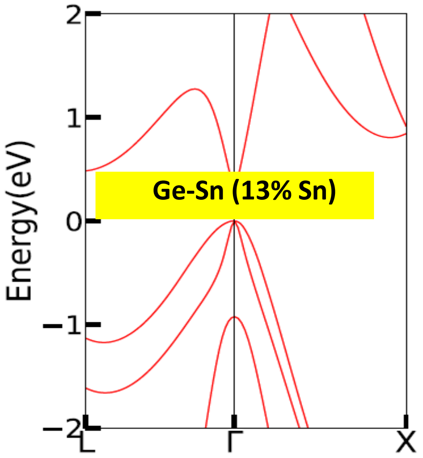

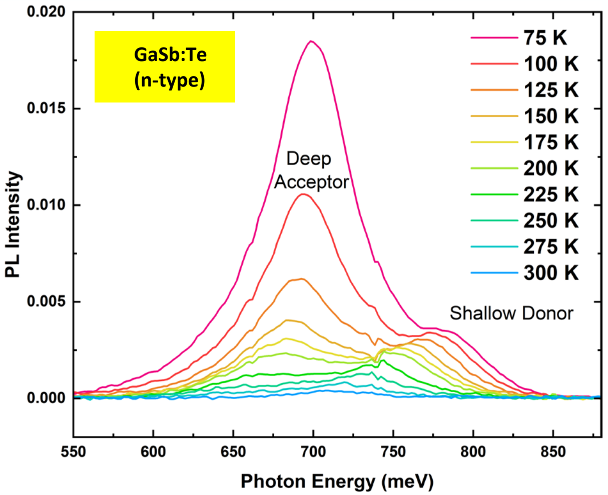

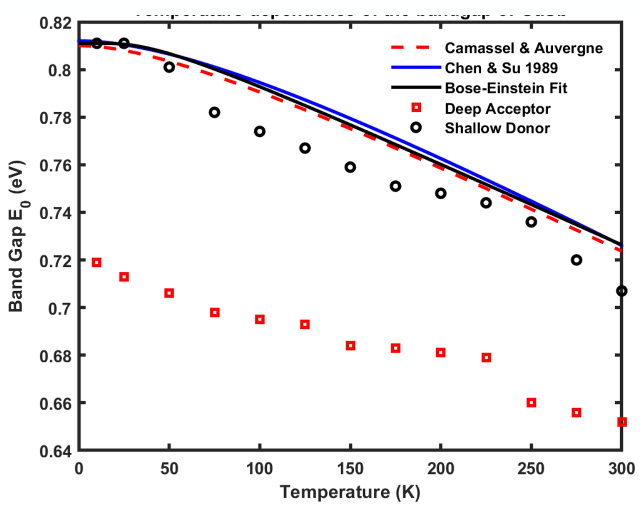

GaSb is a model system for Ge-Sn (with 13% Sn).

Similar conduction band structure.

Photoluminescence:

deep acceptors, shallow donors.

Band gap redshifts with increasing temperature.

Electrons populate Γ- and L-valleys.

Temperature dependence of PL intensity due to activated acceptors and donors (Arrhenius plot).

What's next: pressure + temperature

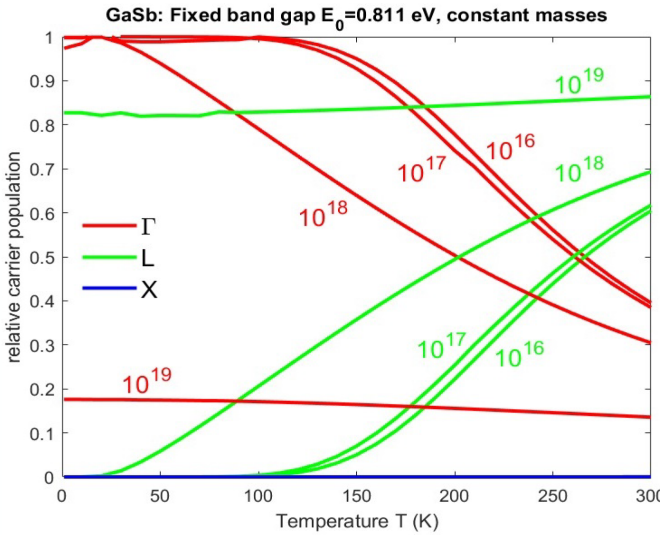

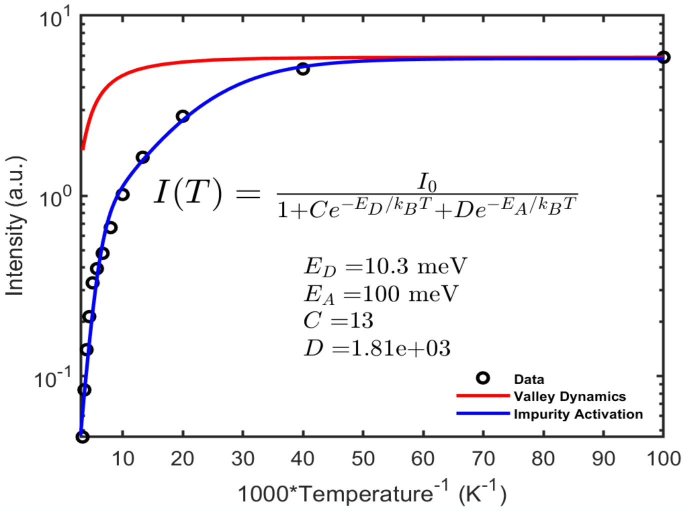

Sonam Yadav, Jaden Love, NMSU

AFRL/RVSU (FA9453-23-2-0001), SCALE

Thermal annealing and oxidation of Ge (100) *and Ge-Sn alloys*

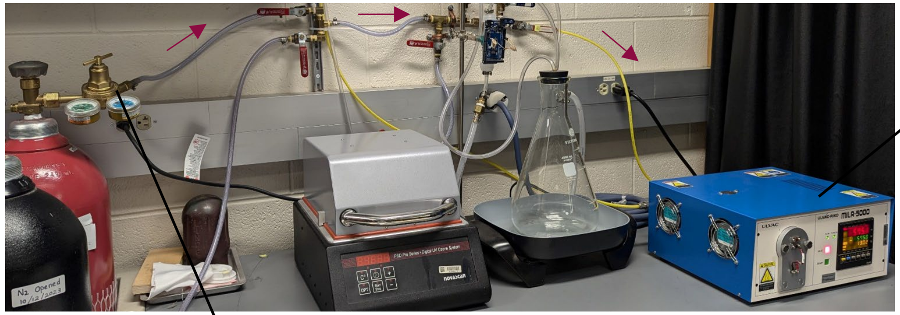

Oxygen Tank and Pressure Gauge

MILA-5000
Rapid Thermal
Annealer (RTA)

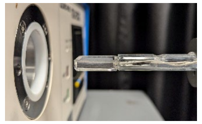

Susceptor
(Sample stage)

E5AR-T Controller

Flow Rate Gauge

Procedures

- Ultrasonically clean in fresh deionized water for 20 min, dry with nitrogen: <1 nm native oxide.
- Anneal in RTA for 1 hour at 550°C under 40 psi pressure and 0.2 l/m dry O_2 flow rate.

Next steps

- Temperature window: ±25C
- Thicker films (longer anneals)
- Study Ge-O lattice vibrations

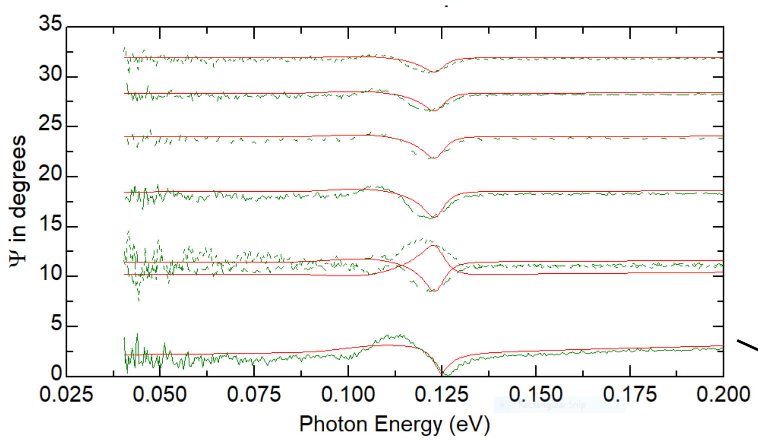

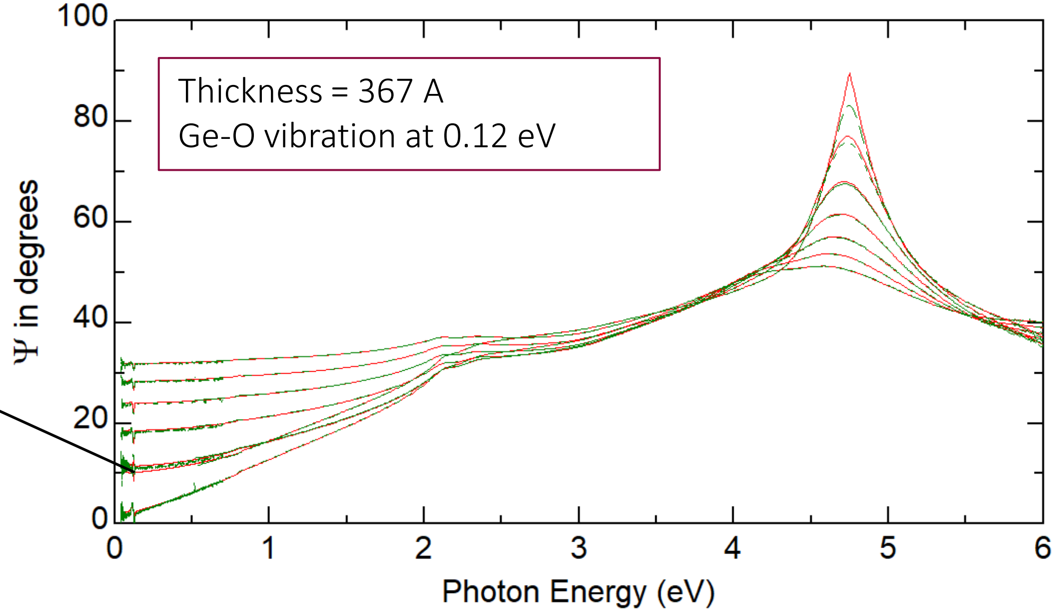

NM STATE

BE BOLD. Shape the Future.

Dani Ortega, Haley Woolf, NMSU; John Kouvetakis, ASU

NSF (DMR-2235447, DMR-2423992), DOD SCALE

Nonparabolicity of InSb conduction band from k·p theory

Kane 8x8 k·p Hamiltonian:

$$\tilde{H}_{\vec{k}} = \begin{pmatrix} E_0 & 0 & -\frac{\hbar\vec{k}}{m_0}iP & 0 \\ 0 & -\frac{2\Delta_0}{3} & \frac{\sqrt{2}\Delta_0}{3} & 0 \\ \frac{\hbar\vec{k}}{m_0}iP & \frac{\sqrt{2}\Delta_0}{3} & -\frac{\Delta_0}{3} & 0 \\ 0 & 0 & 0 & 0 \end{pmatrix}$$

Energy versus k^2

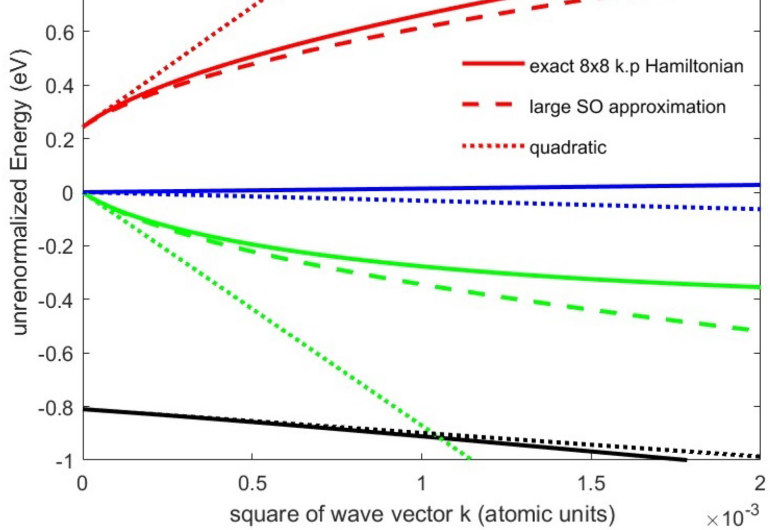

Cubic characteristic equation (solid):

$$\tilde{E}(\tilde{E}-E_0)(\tilde{E}+\Delta_0)-\frac{\hbar^2k^2E_P}{2m_0}\left(\tilde{E}+\frac{2\Delta_0}{3}\right)=0$$

Large spin-orbit approximation (dashed):

$$E_{3,4}=\frac{\hbar^2k^2}{2m_0}+\frac{E_0}{2}\left(1\pm\sqrt{1+\frac{\hbar^2k^2}{2m_0}\frac{2}{\mu_{lh}E_0}}\right)$$

Kane, J. Phys. Chem. Solids **1**, 249 (1957).

Density of CB states

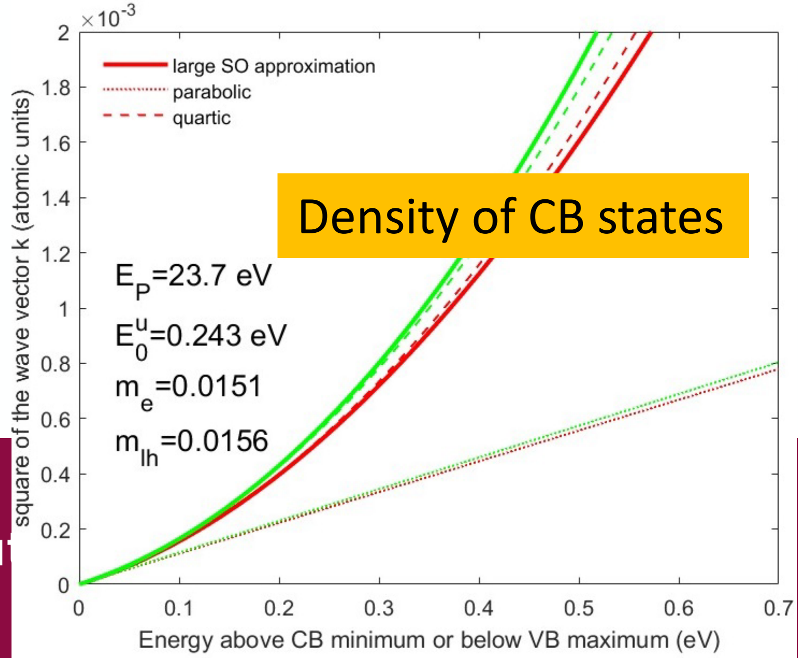

Intrinsic carrier concentration
$n=2\times10^{18}$ cm^{-3} at 800 K

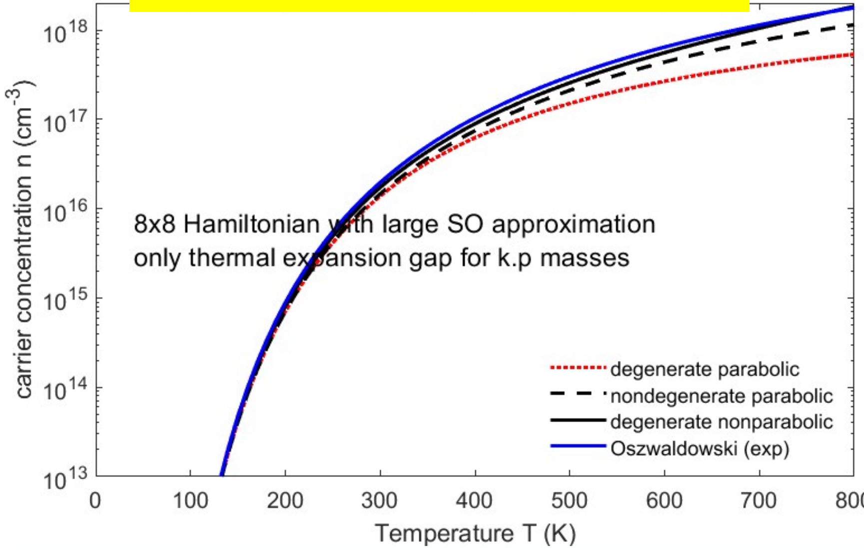

$$\frac{\hbar^2k^2}{2m_0m^*}=\varepsilon(1+\alpha\varepsilon+\beta\epsilon^2)$$

$$\alpha=\frac{(1-m^*)^2}{E_0}$$

Stefan Zollner, NMSU
FA9550-20-1-0135, SFFP
Web: http://femto.nmsu.edu

Infrared absorption of α-tin at the direct band gap

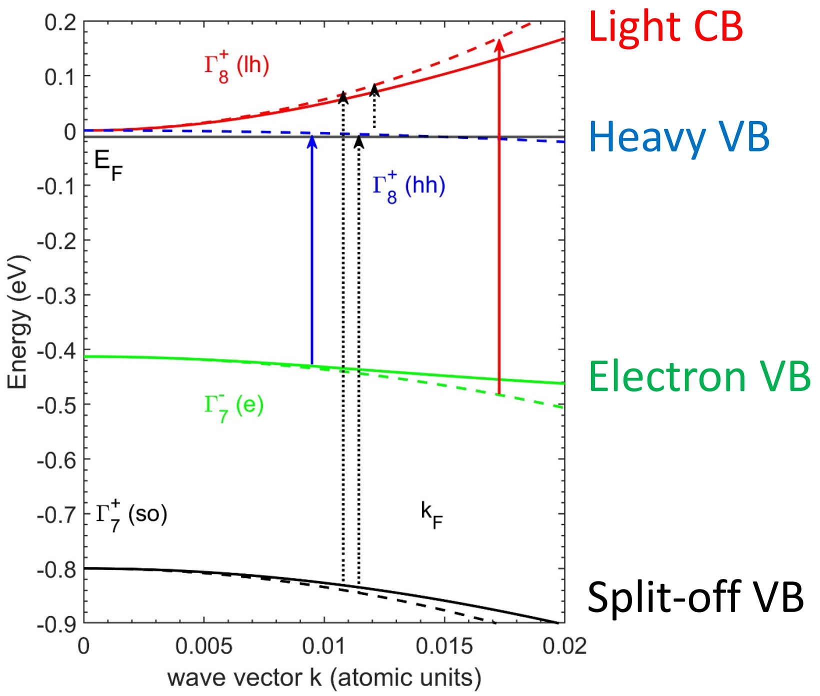

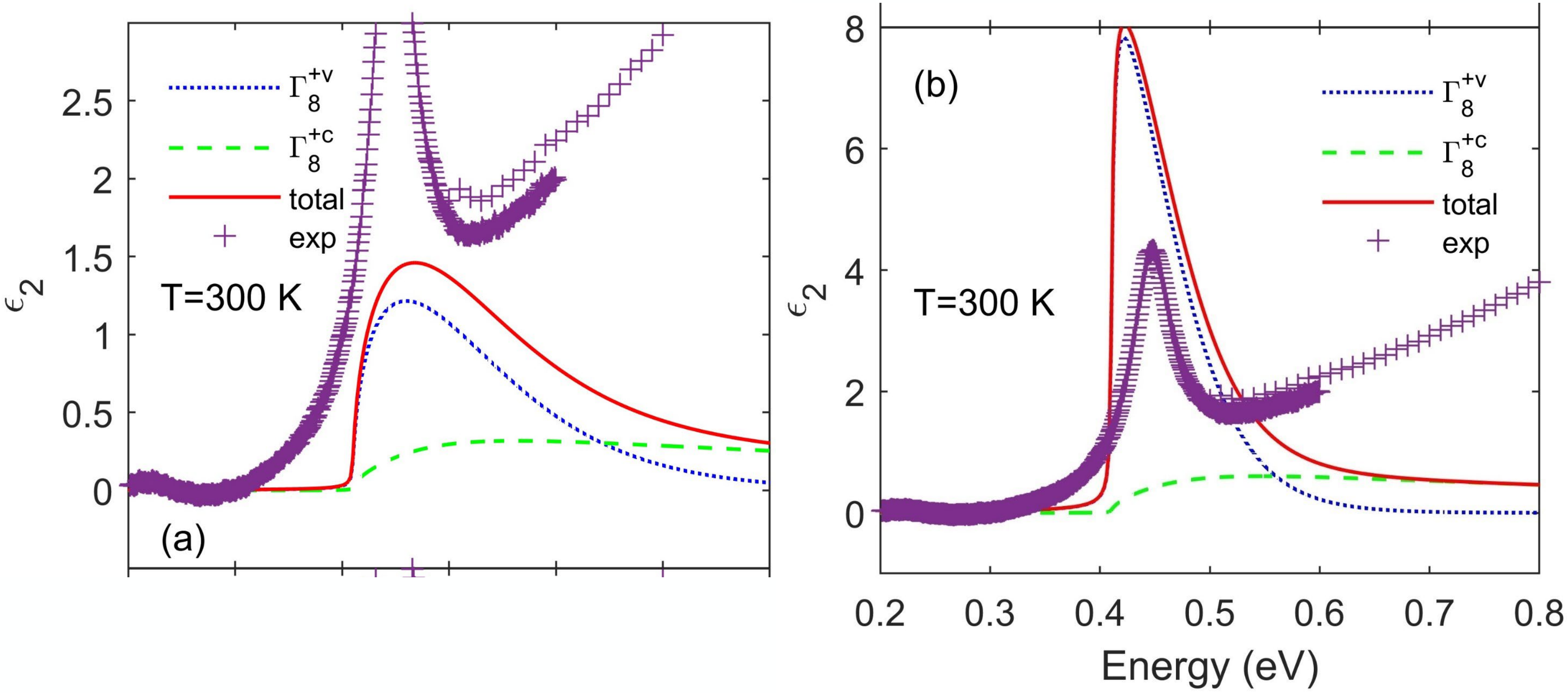

Parabolic bands: dashed
Kane 8x8 k.p bands: solid
Chemical potential: μ=–12.5 meV at 300 K
Intrinsic: n=p=3.7x10^{18} cm^{-3} at 300 K

Parabolic bands
No excitonic enhancement
Compare Carrasco (2018)

Nonparabolic bands
With screened excitonic enhancement
Fine-tune mass for better agreement.

Stefan Zollner, NMSU; JVST B **42**, 022203 (2024)
FA9550-20-1-013, SFFP

Low-temperature ellipsometry with a recirculating He cooler

- Ellipsometric angles Ψ and Δ of one-side polished NiO (111) on J. A. Woollam IR VASE Mark II ellipsometer with ST-400 cryostat.
- NiO as a test case for infrared ellipsometry. a-tin will be next.
- Liquid He was used to cool down the sample to 25 K. Heat up to 500 K in same chamber.

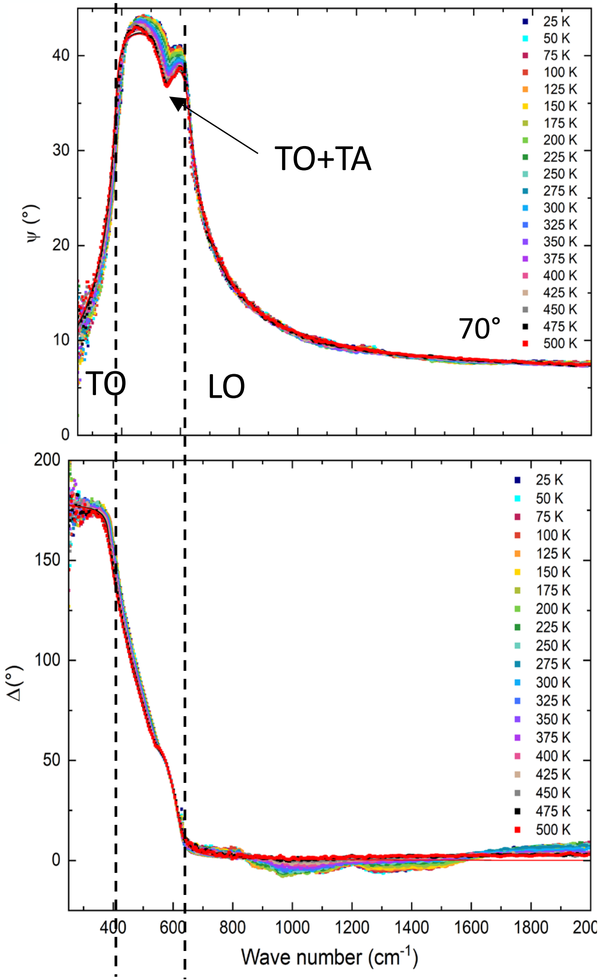

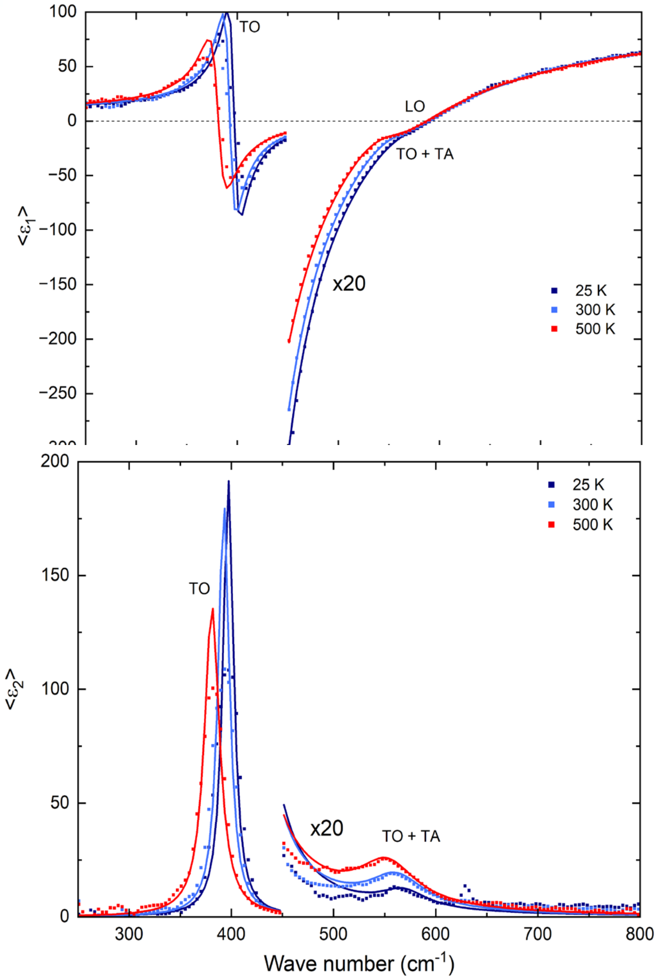

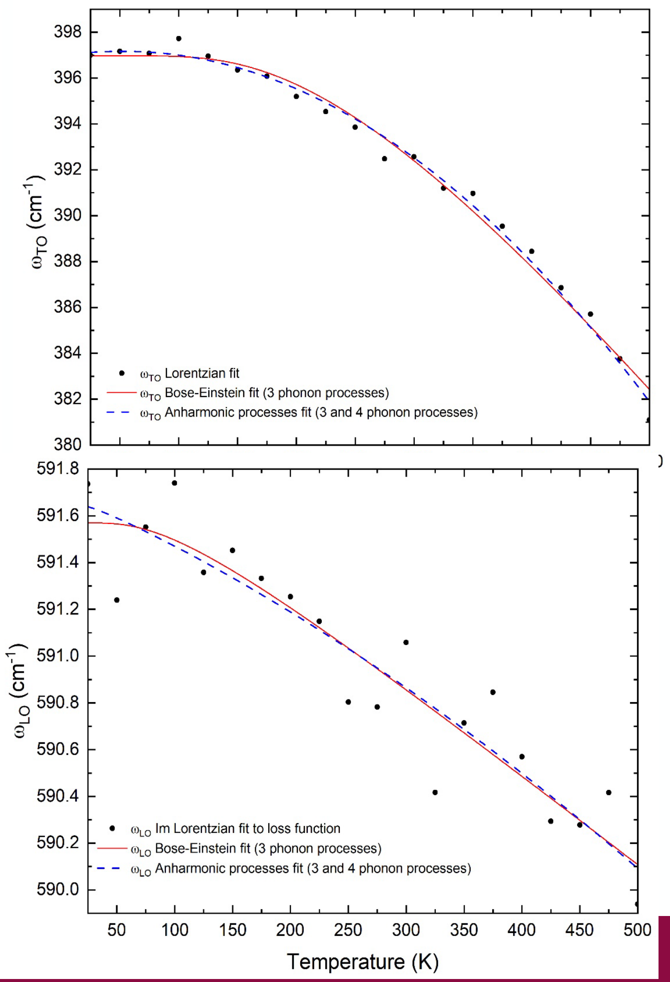

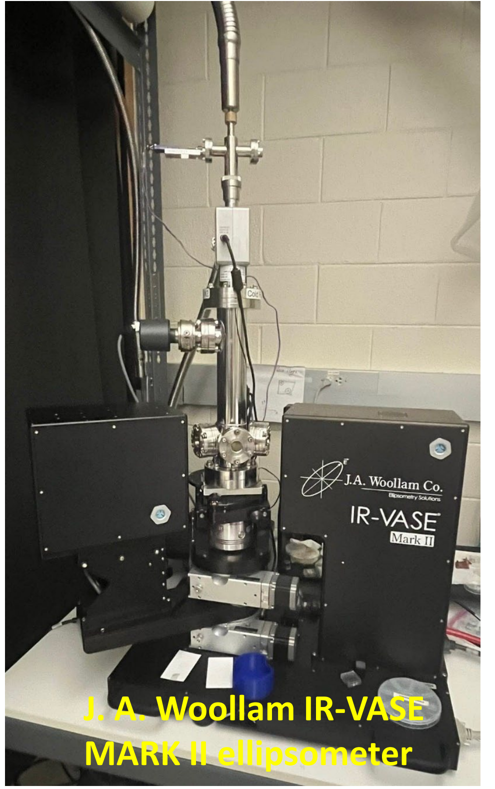

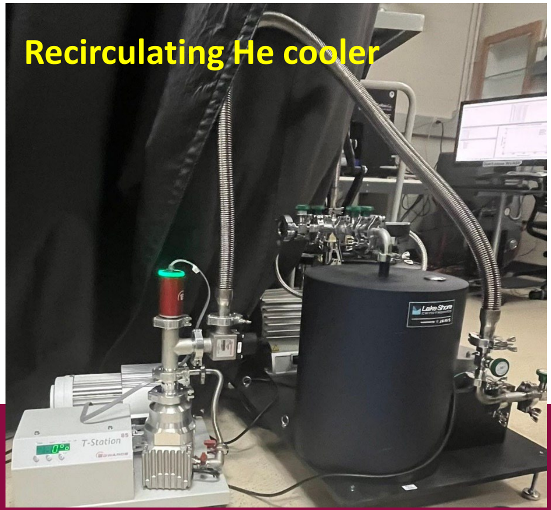

Yoshitha Hettige, Jaden Love, Atlantis Moses, NMSU

ARO (W911NF-22-2-0130), DOD SCALE

Direct-gap infrared absorption of α-Sn (temperature-dependent)

α-Sn Band Structure

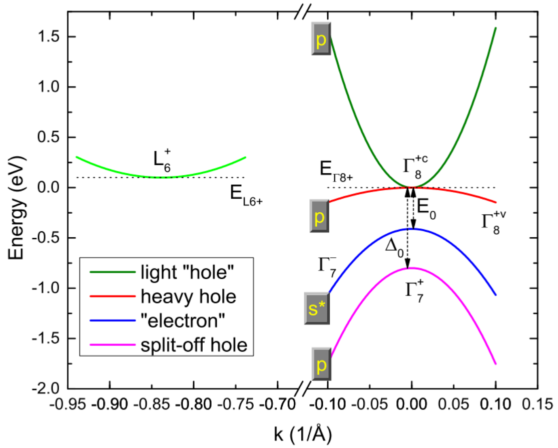

- Pseudomorphic α-Sn on InSb or CdTe has a strong E_0 peak at 0.41 eV.
- α-Sn on InSb: temperature-independent. Doped with In from substrate
- α-Sn on CdTe: amplitude increases with increasing temperature (thermal activation of carriers).
- Unintentional doping of α-Sn with In may by due to differences in sample preparation.

- **Growth on Sb-terminated InSb looks like growth on CdTe.**
- Low intrinsic carrier concentration at low T, increases at 300 K.
- Signal to noise ratio will be improved.
- Need calibration of window effects and data analysis.

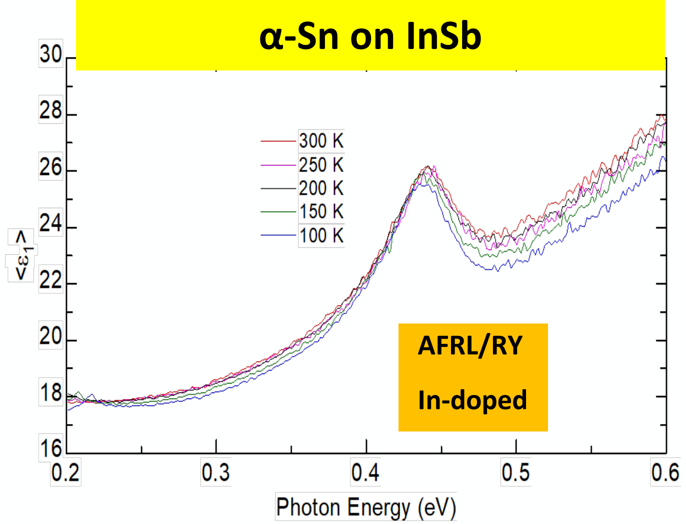

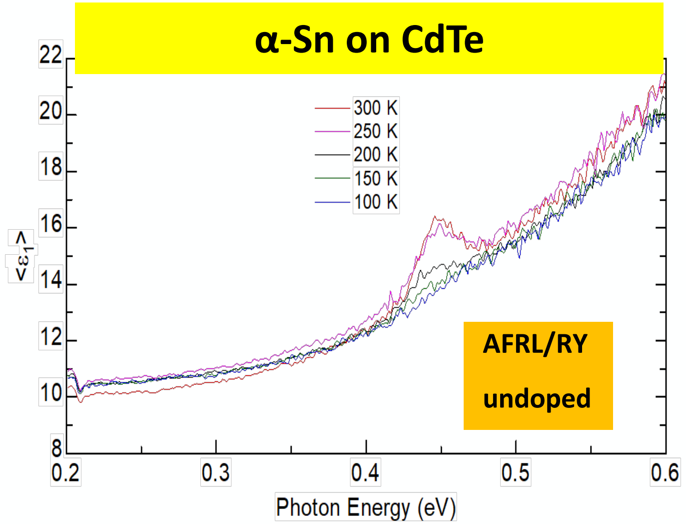

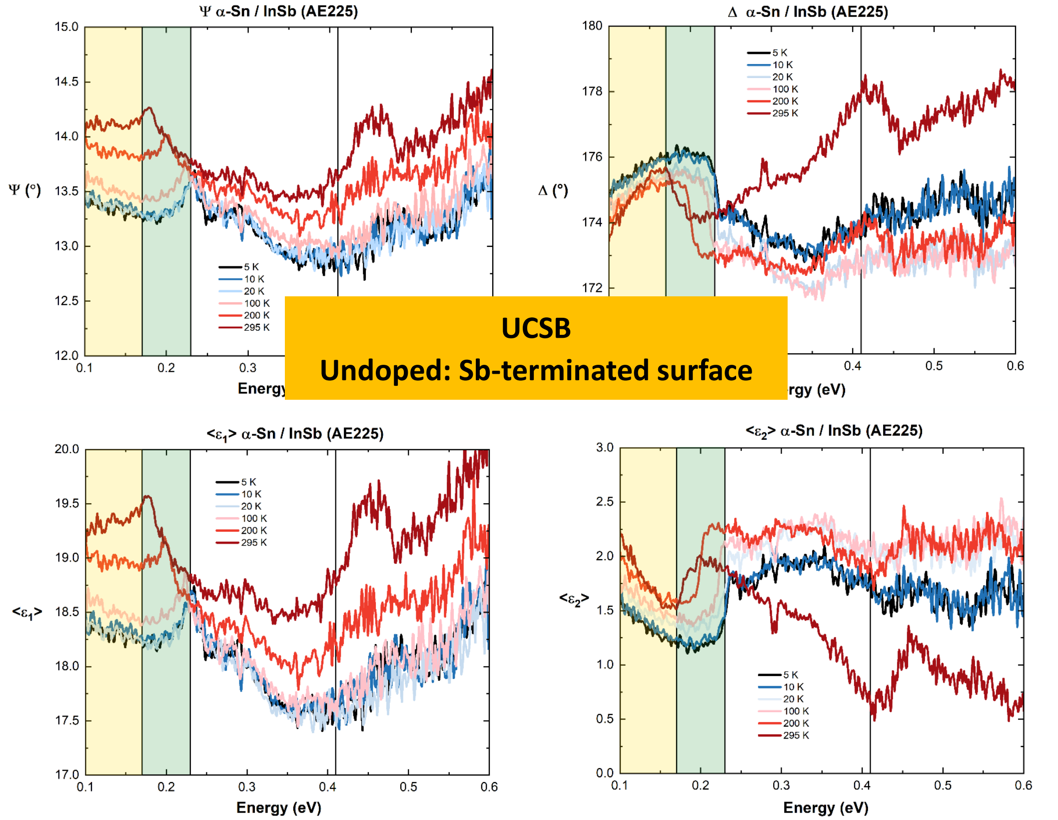

Carrasco, APL 113, 232104 (2018)

Jaden Love, NMSU; Aaron Engel, Chris Palmstrom, UCSB

NSF (DMR-2423992), DOD SCALE

Excitonic enhancement of optical transitions

Excitonic Rydberg energy

$$R = \frac{\mu}{m_0 \varepsilon_r^2} R_H$$

Discrete states

$$E_n = E_g - \frac{1}{n^2} R_X$$

Discrete absorption

$$\varepsilon_2(E) = \frac{8\pi |P|^2 \mu^3}{3\omega^2 (4\pi\varepsilon_0)^3 \varepsilon_r^3} \sum_{n=1}^{\infty} \frac{1}{n^3} \delta(E - E_n)$$

Continuum absorption

$$\varepsilon_2(E) = \frac{2|P|^2 (2\mu)^{3/2} \sqrt{E - E_0}}{3\omega^2} \frac{\xi e^{\xi}}{\sinh \xi}$$

$$\xi = \pi \sqrt{R / E - E_0}$$

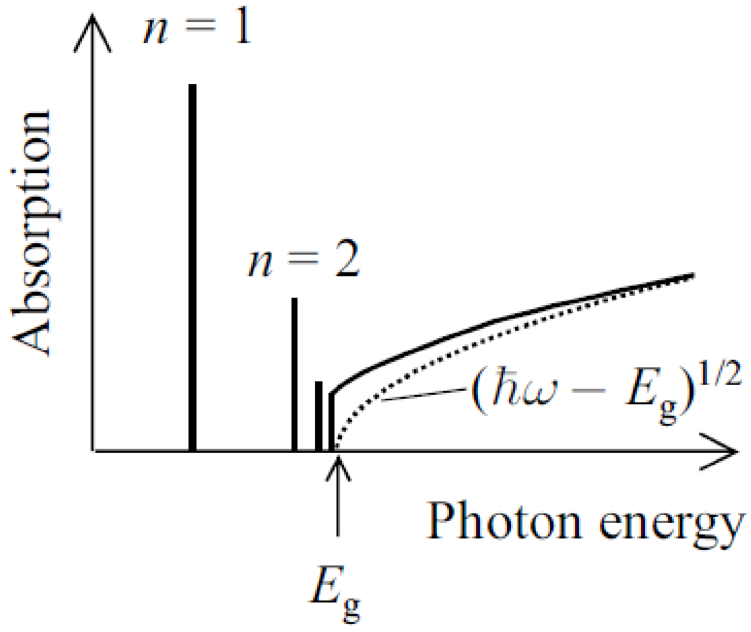

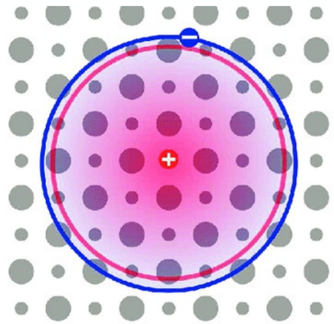

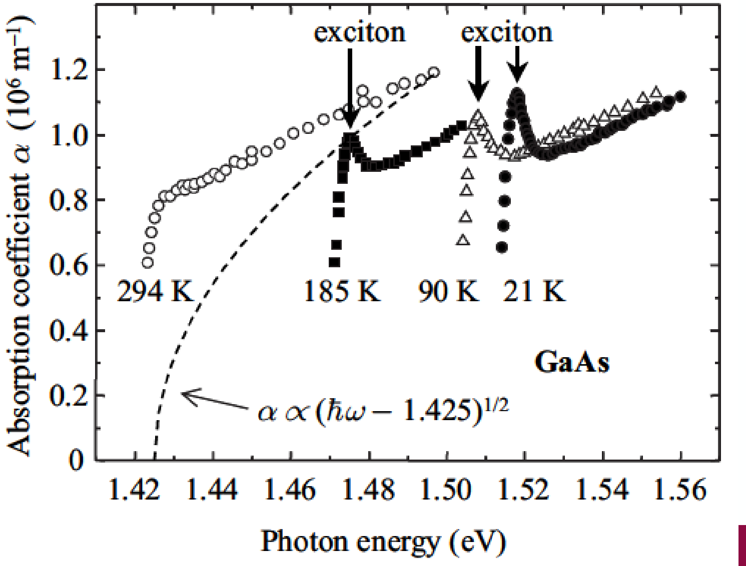

Use Bohr wave functions to calculate ε_2.
Toyozawa discusses broadening.

R. J. Elliott, Phys. Rev. **108**, 1384 (1957)
Yu & Cardona; Fox, Chapter 4

Two-dimensional Bohr problem

$$H = -\frac{\hbar^2}{2\mu_\perp}\left(\frac{\partial^2}{\partial x^2}+\frac{\partial^2}{\partial y^2}\right) - \frac{\hbar^2}{2\mu_\parallel}\frac{\partial^2}{\partial z^2} - \frac{e^2}{\varepsilon_r r}$$

Assume that $\mu_{||}$ is infinite (separate term).
Use cylindrical coordinates.
Separate radial and polar variables.
Similar Laguerre solution as 3D Bohr problem.

$$a_X = \frac{4\pi\varepsilon_0\varepsilon_r\hbar^2 m_0}{\mu_\perp \mu e^2}$$

$$R = \frac{\mu_\perp e^4}{2\hbar^2 m_0 (4\pi\varepsilon_0\varepsilon_r)^2}$$

$$E_n = -\frac{R}{\left(n-\frac{1}{2}\right)^2}, \qquad n = 1,2,\ldots$$

Half-integral quantum numbers

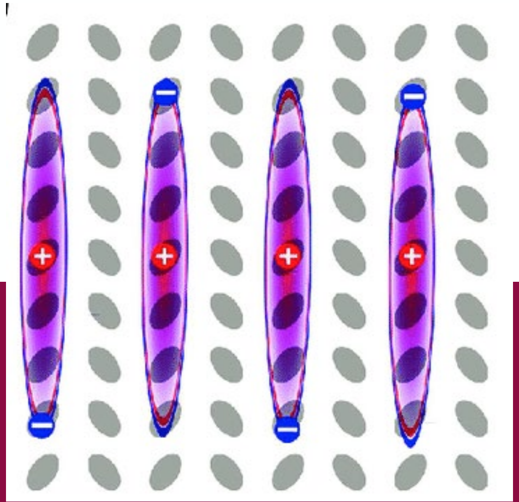

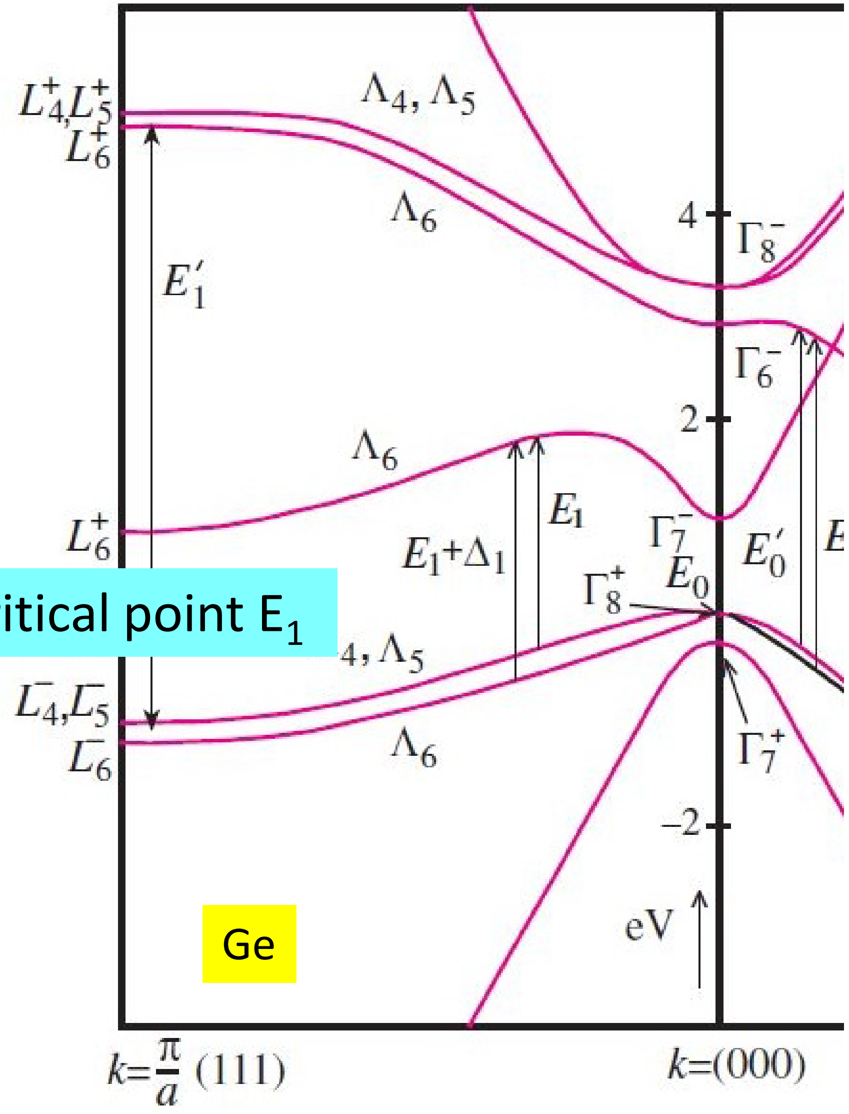

2D critical point E_1

M. Shinada and S. Sugano, J. Phys. Soc. Jpn. **21**, 1936 (1966).

Comparison with experimental data

$$\varepsilon(E, E_1, \Gamma, R, k_{\max}) = \frac{k_{\max} e^2 \bar{P}^2 \mu_\perp^{(E_1)}}{3\varepsilon_0 m^2 \pi (E + i\Gamma)^2} \left\{ g_a \left[\sqrt{\frac{R}{E_1 - (E + i\Gamma)}} \right] + g_a \left[\sqrt{\frac{R}{E_1 - (-E - i\Gamma)}} \right] - 2 g_a \left[\sqrt{\frac{R}{E_1 - (0)}} \right] \right\}$$

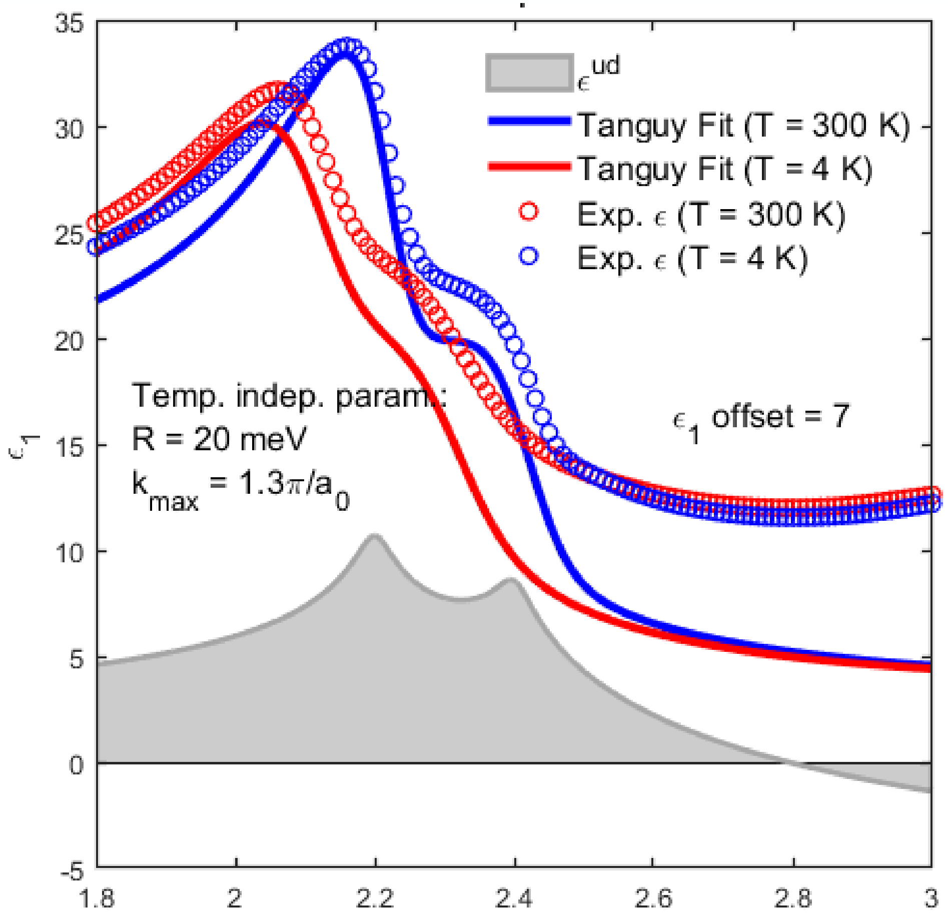

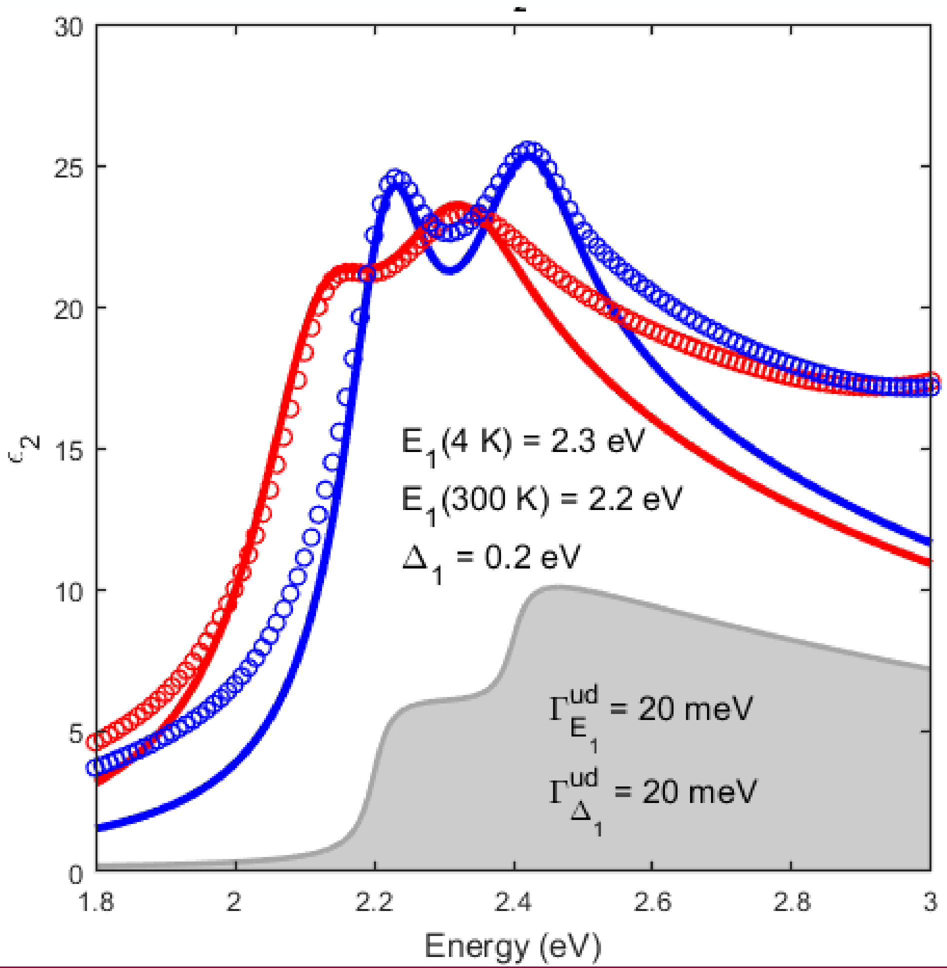

Tanguy 2D

Experimental data:

Emminger (5 K), JVST B **38**, 012202 (2020).

Nunley (300 K), JVST B **34**, 061205 (2016)

Carlos Armenta, NMSU
AFOSR (FA9550-24-1-0061)

Experimental setup: pump-probe ellipsometry

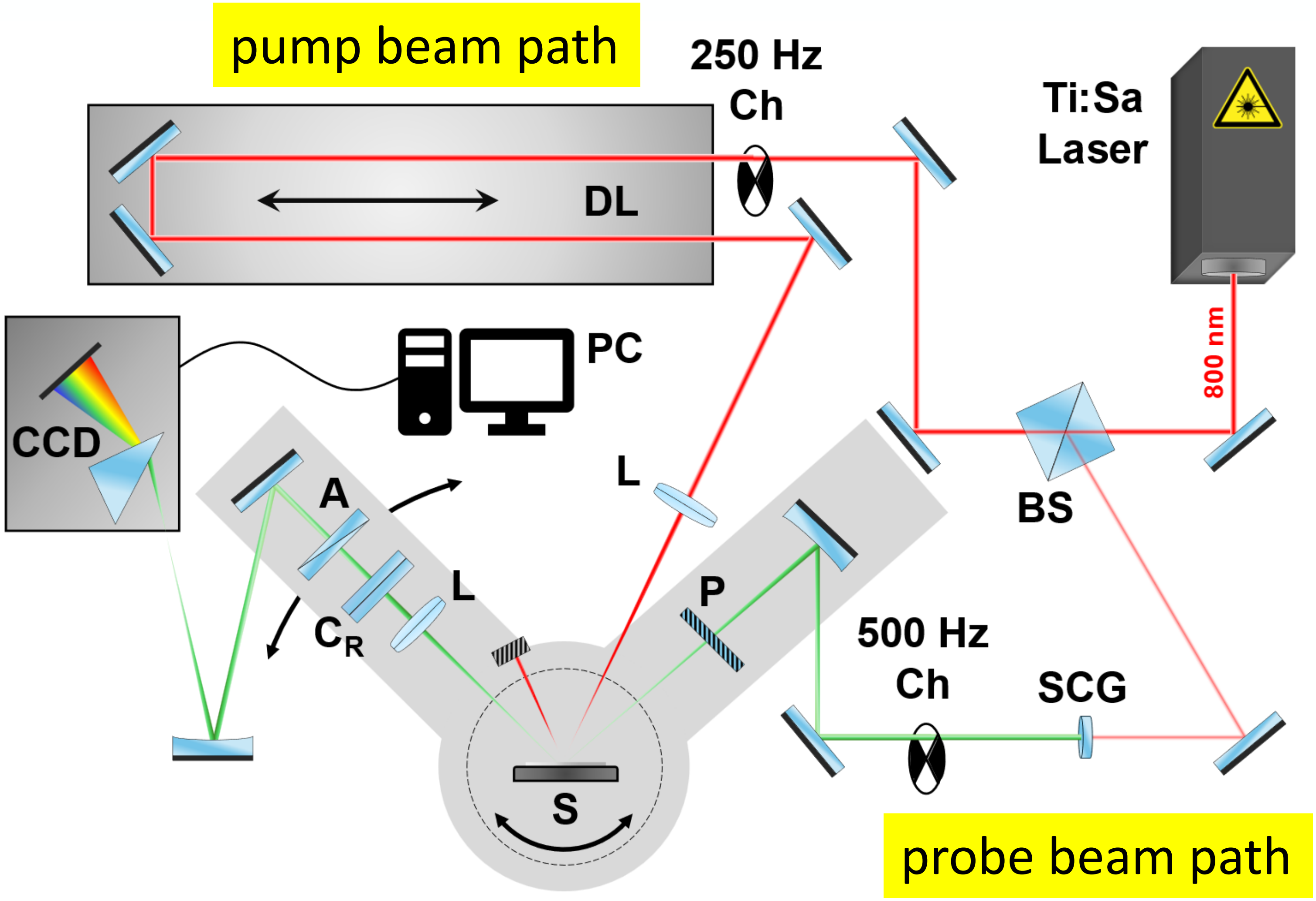

Ch: Chopper (500 Hz, 250 Hz)

A: Analyzer

P: Polarizer

C_R: Rotating Compensator

L: Lens

S: Sample

DL: Delay Line
(~6.67 ns pump-probe delay, 3 fs resolution)

BS: Beam Splitter

SCG: Super-continuum Generation

CCD: Charge-coupled device detector

S. Richter, Rev. Sci. Instrum. **92**, 033104 (2021).
S. Espinoza, Appl. Phys. Lett. **115**, 052105 (2019).
ELI Beamlines, Dolni Bezany, Czech Republic

Set-up: Femtosecond pump-probe ellipsometry

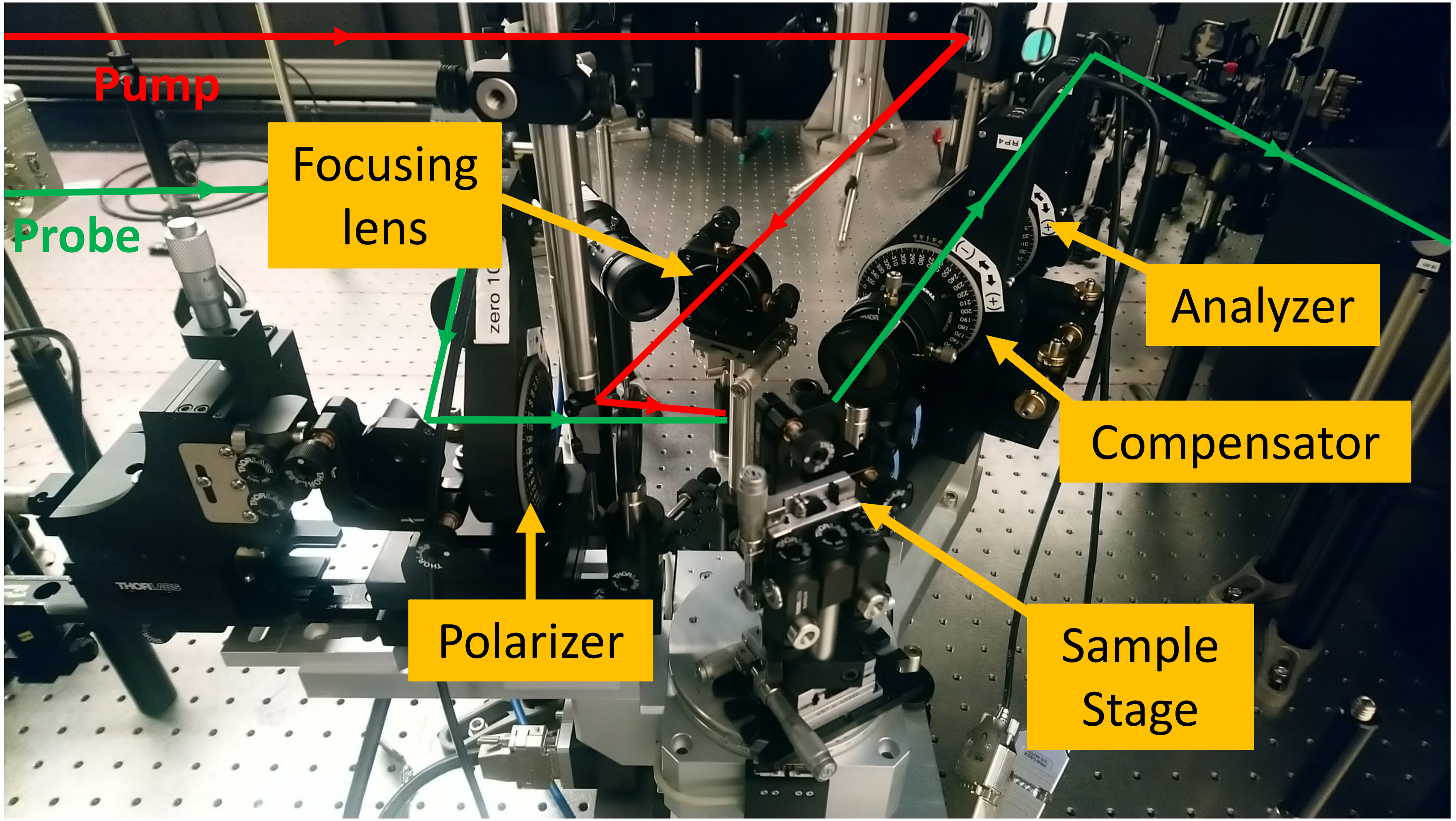

Rotating compensator ellipsometer:

Compensator was rotated in steps of 10° for a total of 55-65 angles.

Probe beam of 350-750 nm at 60° incidence angle.

P-polarized pump beam: 35 fs pulses of 800 nm wavelength at 1 kHz repetition rate.

Delay time from -10 to 50 ps.

Time resolution of about 500 fs.

Espinoza et al., APL **115**, 052105 (2019)
ELI Beamlines, Dolni Bezany, Czech Republic

Pseudo-dielectric function of Ge versus of delay time

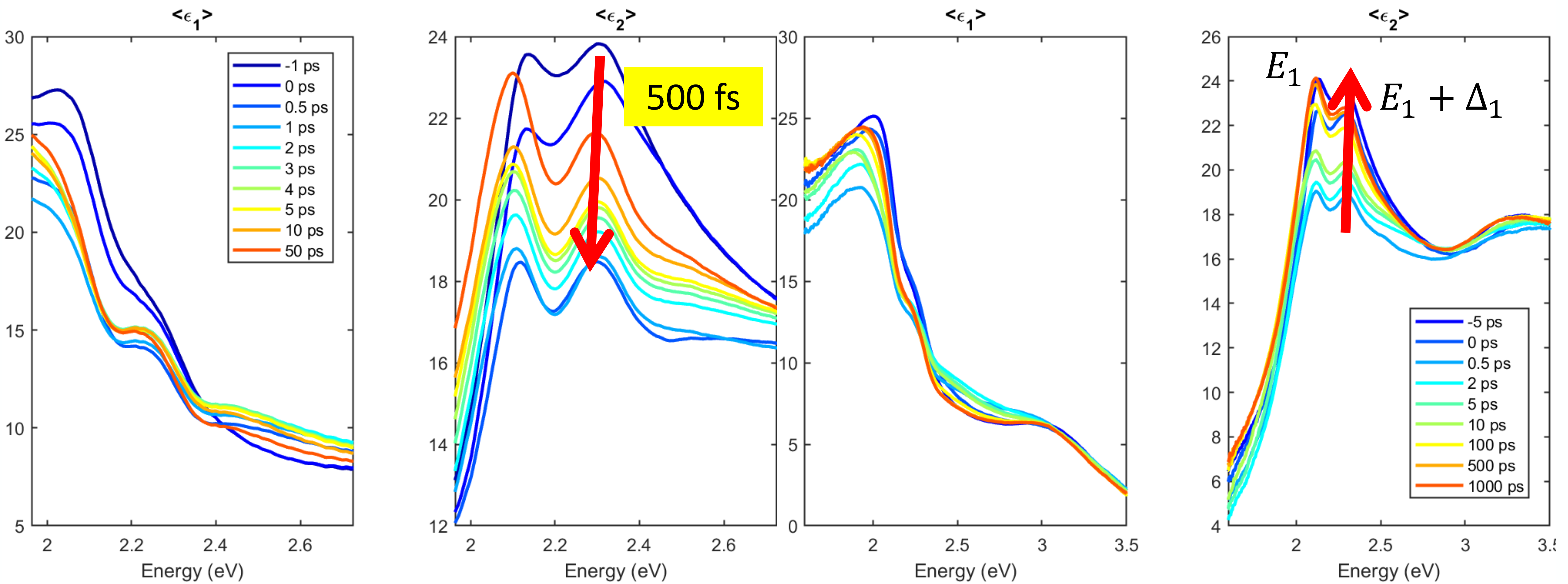

Rapid decrease of ε within first 500 fs.

Recovery takes 1 ns or longer.

Carlos Armenta, NMSU
AFOSR (FA9550-24-1-0061)

Carrier relaxation (<100 fs): Energy transfer to lattice

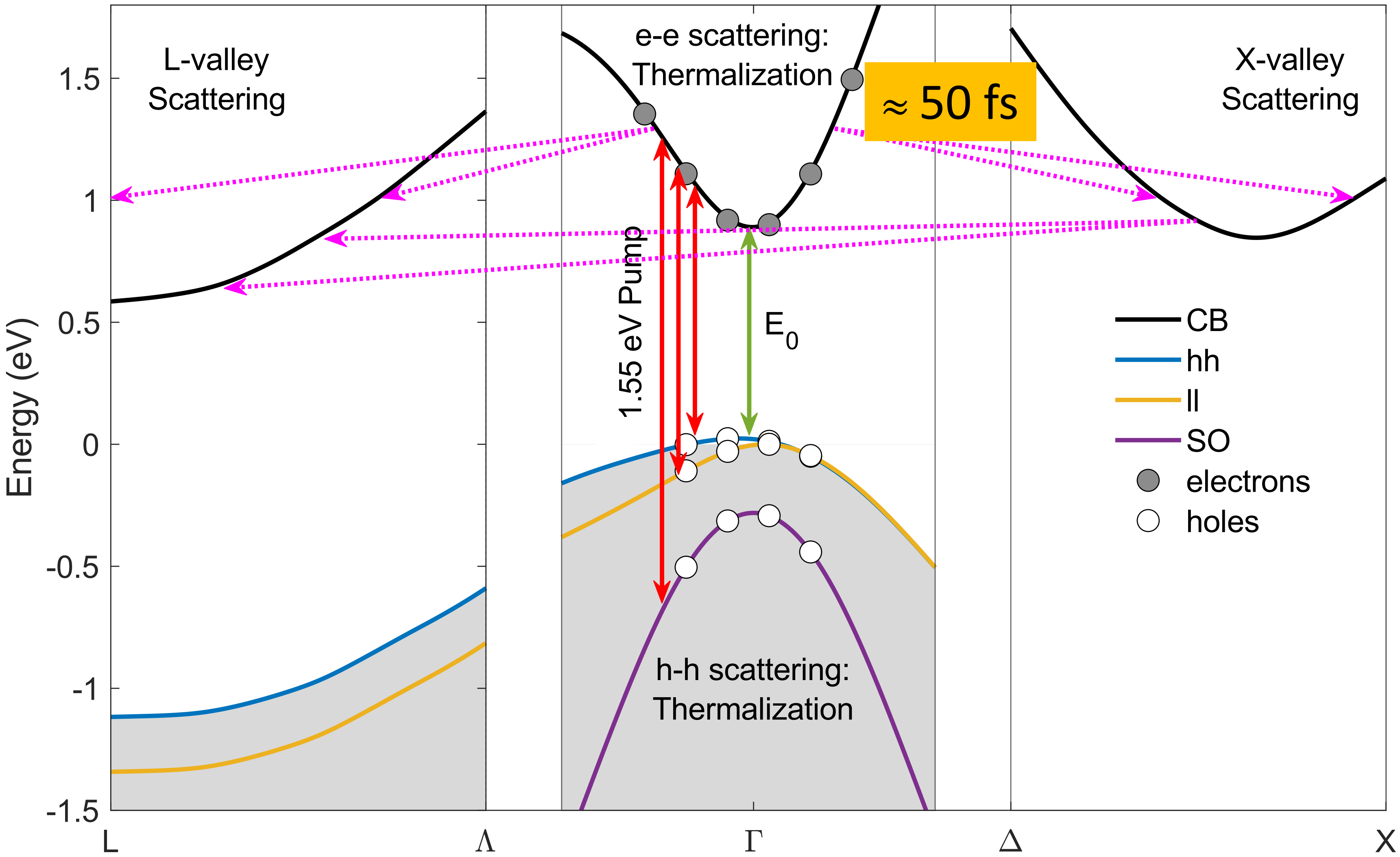

$$\varepsilon = \frac{\hbar\omega_{\mathrm{pump}} - E_0}{1 + m_e/m_h}$$

Plasma temperature:

$$T_{\mathrm{C}} \approx \frac{\varepsilon}{3k_{\mathrm{B}}}$$

ε=0.7 eV

T=2500 K

Intervalley scattering is more efficient than intravalley scattering.

Stefan Zollner, Sudha Gopalan, and Manuel Cardona, Effective **deformation potentials** in the description of time-resolved and hot-electron luminescence, Solid-State Commun. **76**, 877-879 (1990)

Electron concentration from density of states

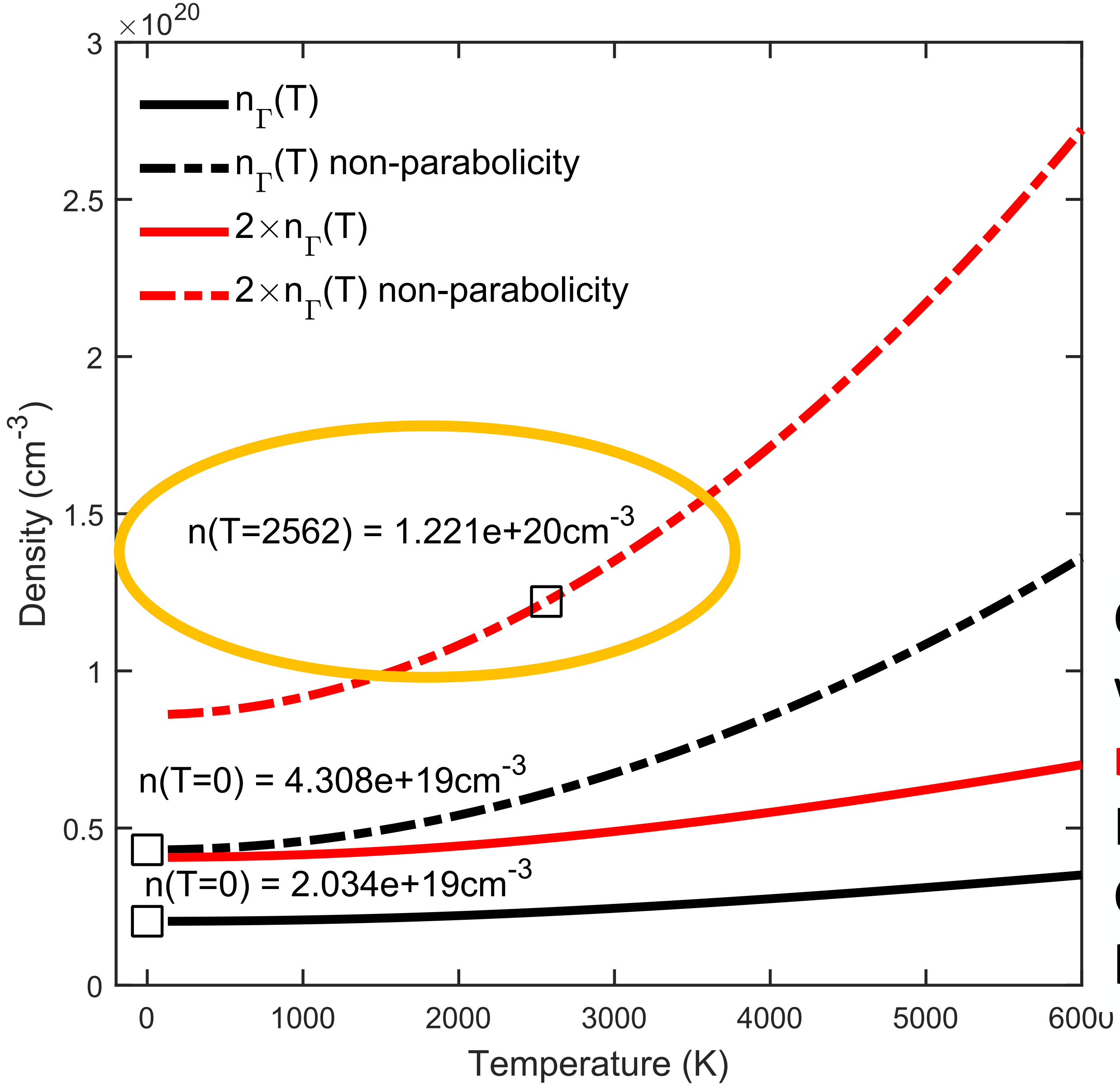

To avoid bleaching of the absorption, the chemical potential μ cannot be larger than the excess electron energy ε. Assume

$\mu = \varepsilon + E_0$

$$n_\Gamma(T) = \frac{1}{4}\left(\frac{2m_{e,\Gamma}k_B T}{\pi\hbar^2}\right)^{3/2} F_{1/2}\left(\frac{\varepsilon}{k_B T}\right)$$

Calculate maximum electron concentration with Fermi-Dirac statistics:

n cannot be more than 10^{20} cm^{-3}.

High above the Mott density (10^{17} cm^{-3}).

Consider density of states with conduction band non-parabolicity from k.p theory.

Electrons cooling by intervalley scattering (>500 fs)

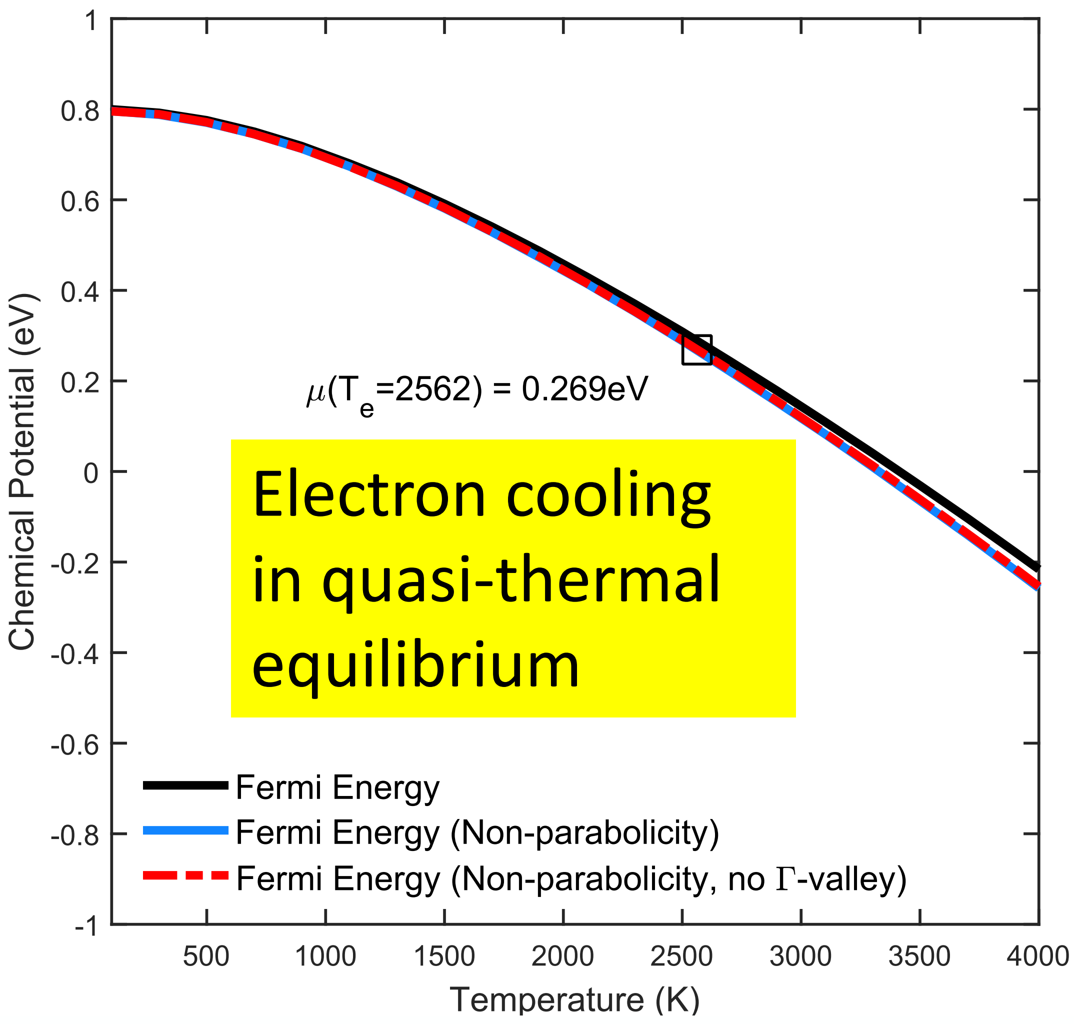

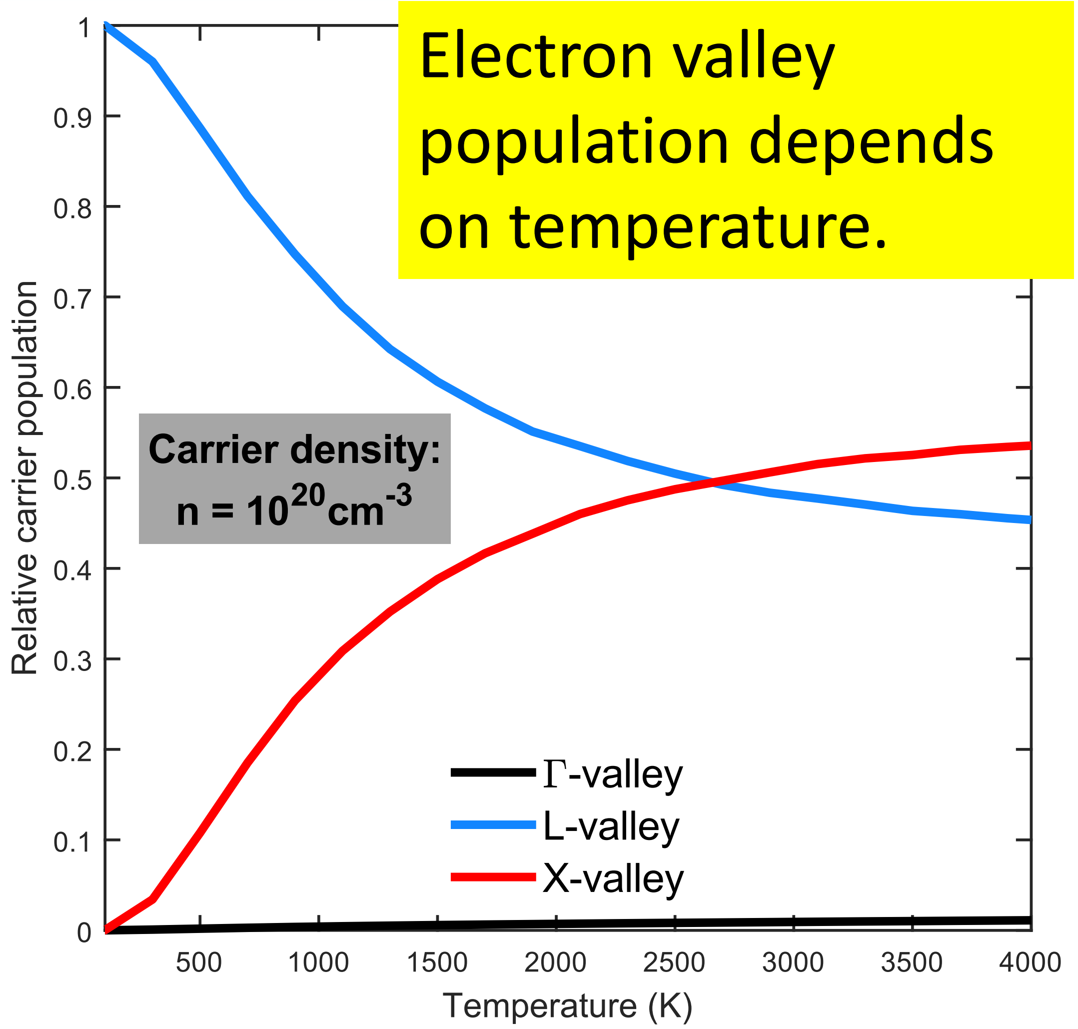

Carlos Armenta, NMSU
AFOSR (FA9550-24-1-0061)

Electrons cooling by intervalley scattering (>500 fs)

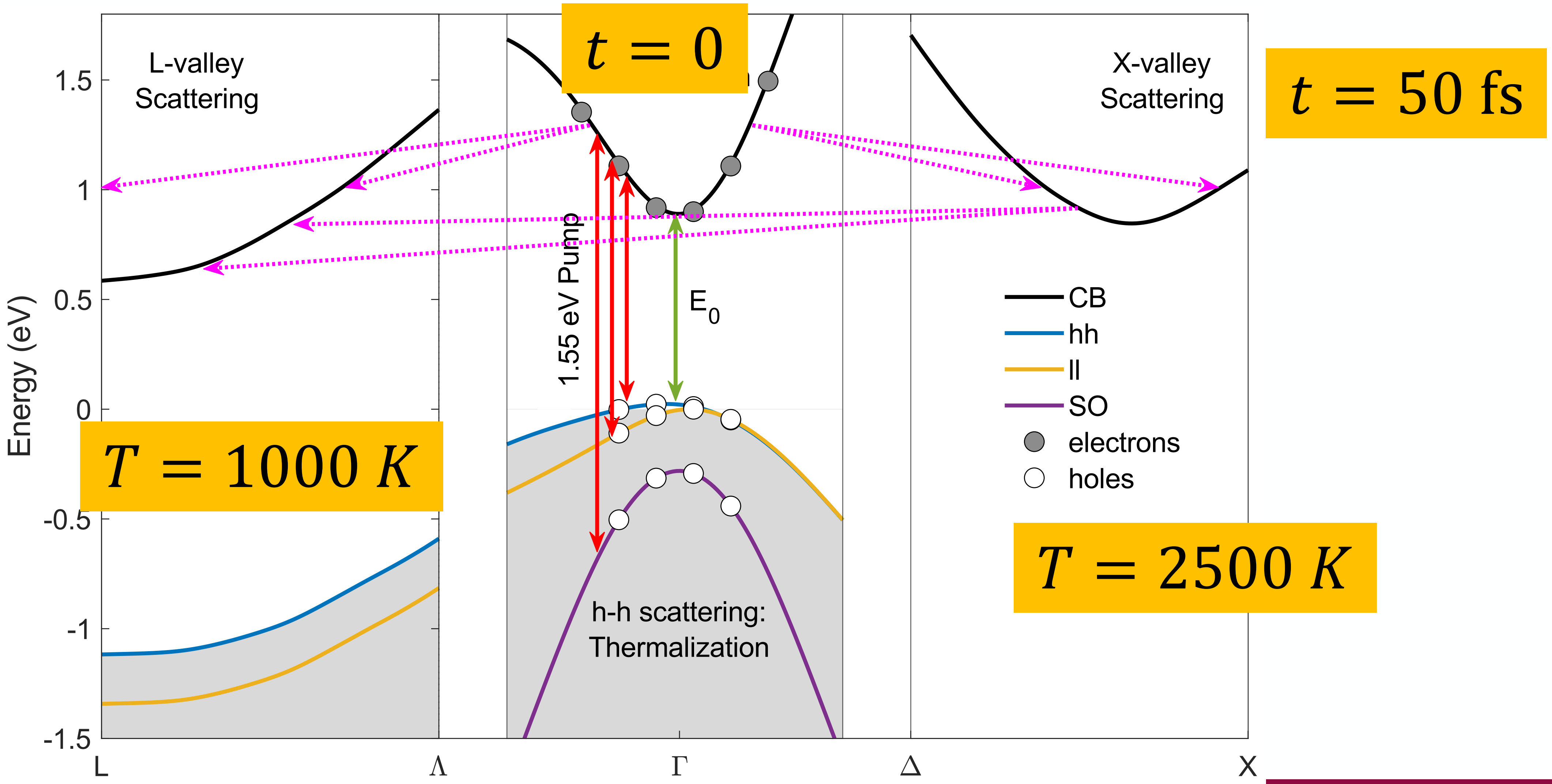

Carlos Armenta, NMSU
AFOSR (FA9550-24-1-0061)

Band-filling model for transient dielectric function

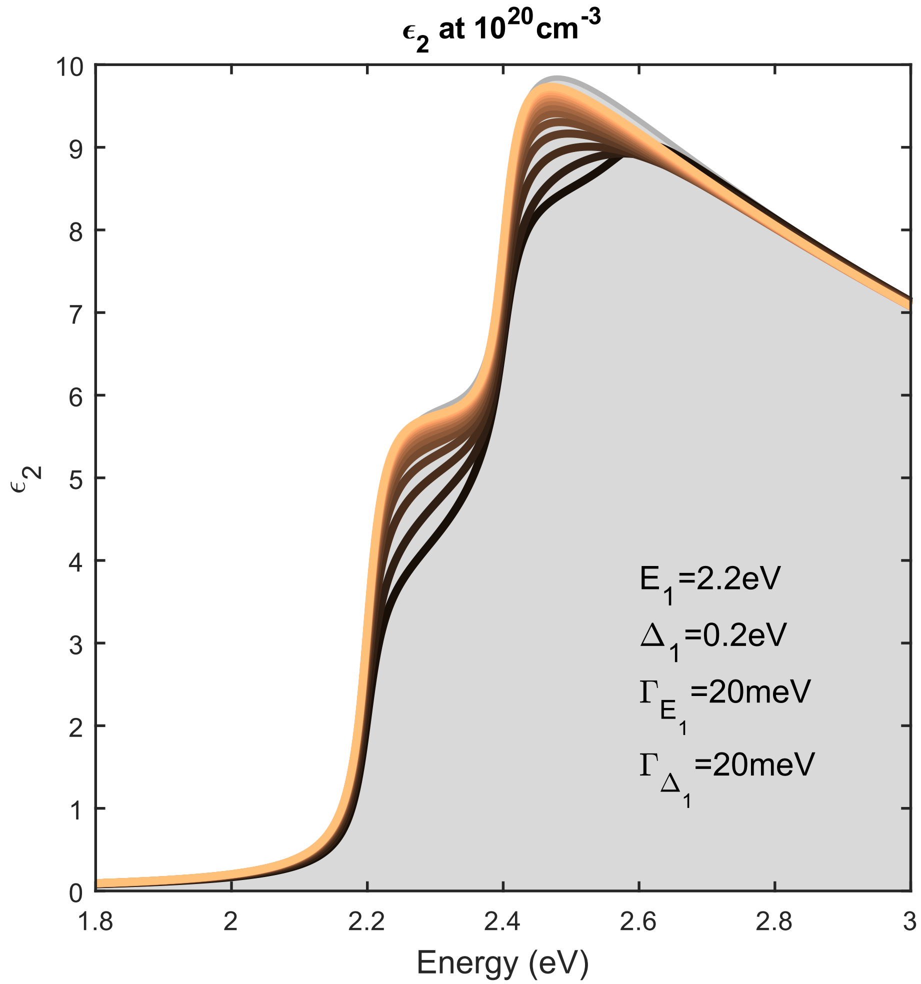

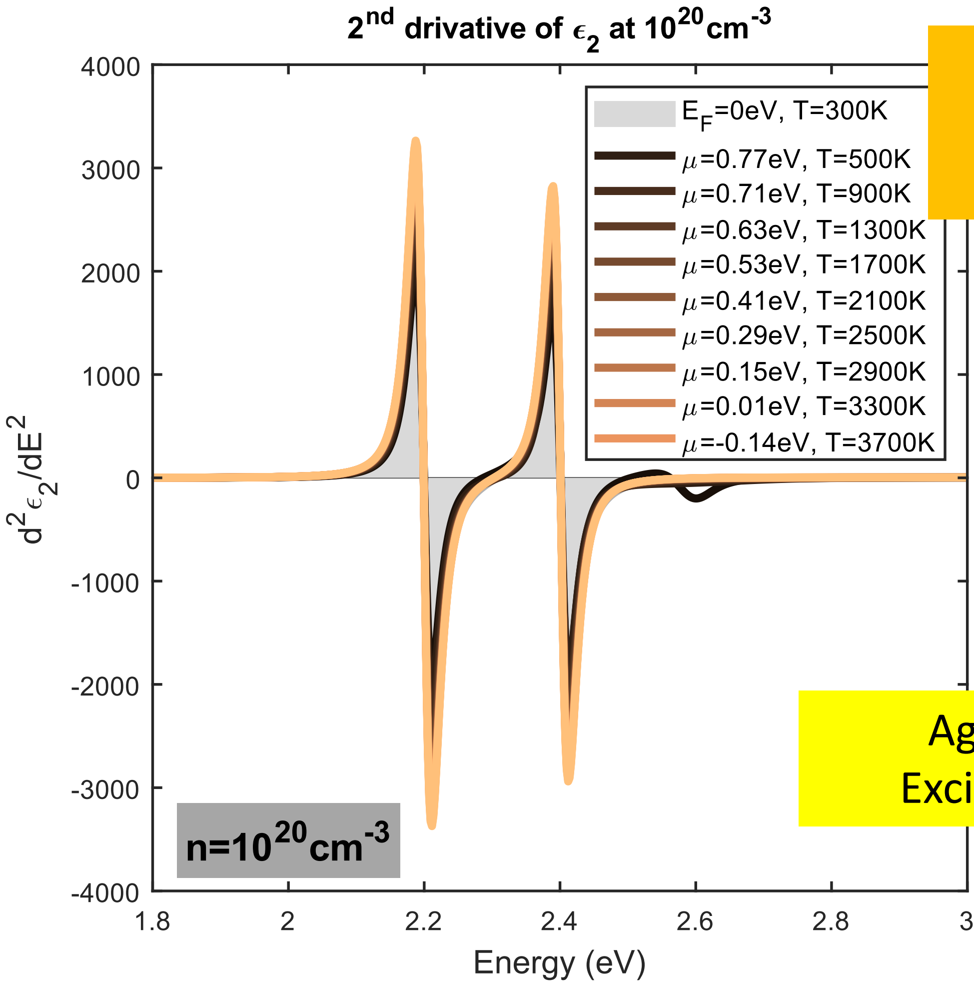

No Burstein-Moss shift for 2D CP:
$\Delta E_{\mathrm{BM}} = 0$

Agreement not good:
Excitonic effects ignored

$$\varepsilon_2(E) = \frac{2e^2\bar{P}^2\mu_\perp}{3\pi\varepsilon_0 m^2 E^2} H(E - E_1) \int_{-k_{\max}}^{k_{\max}} 1 - f[E_c(E, k_z^2)]dk_z$$

Xu, JAP **125**, 085704 (2019).
Xu, PRL **118**, 267402 (2017).

Comparison with experiment: Excitonic effects included, but no screening of 2D excitons (how ???)

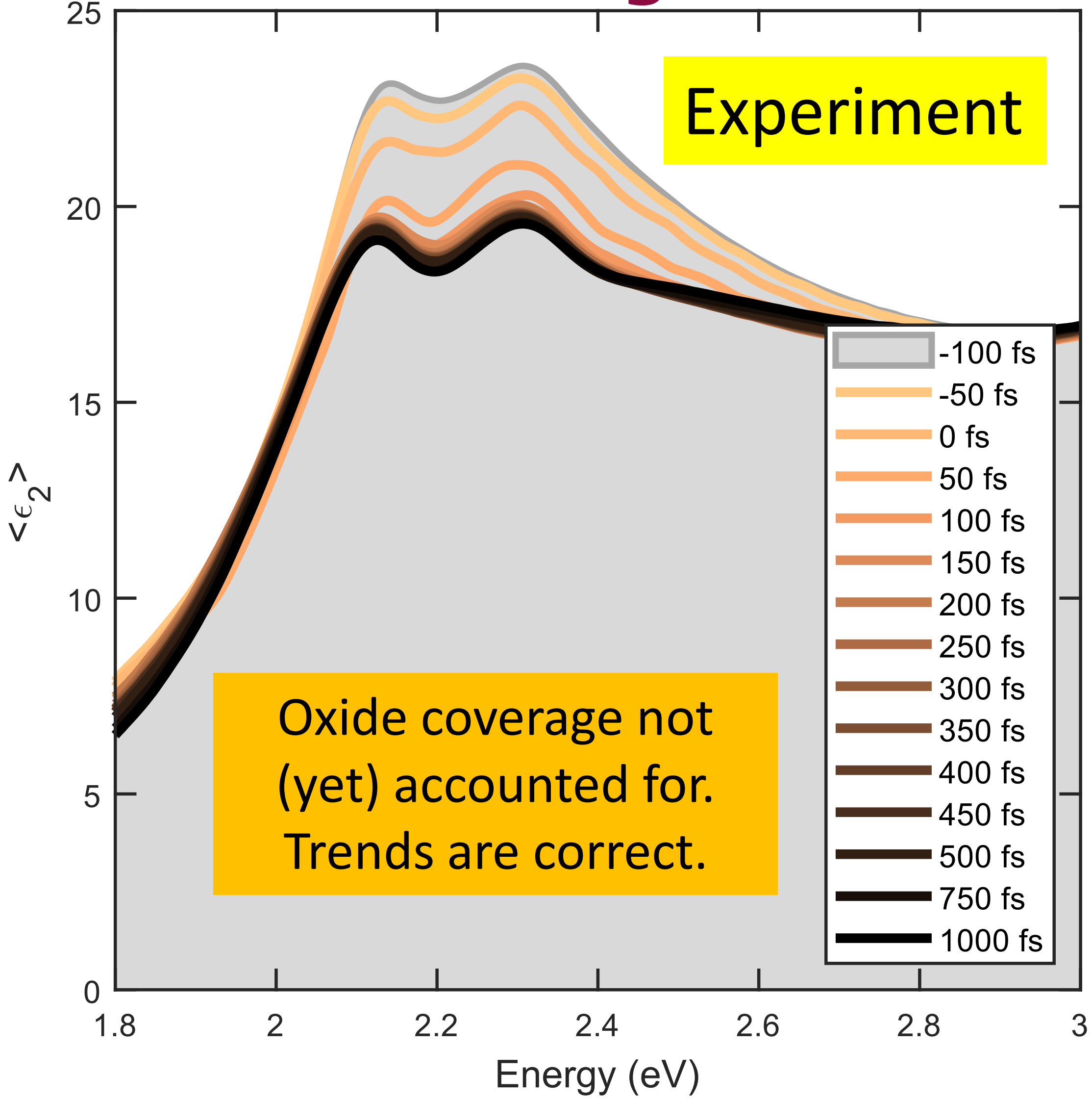

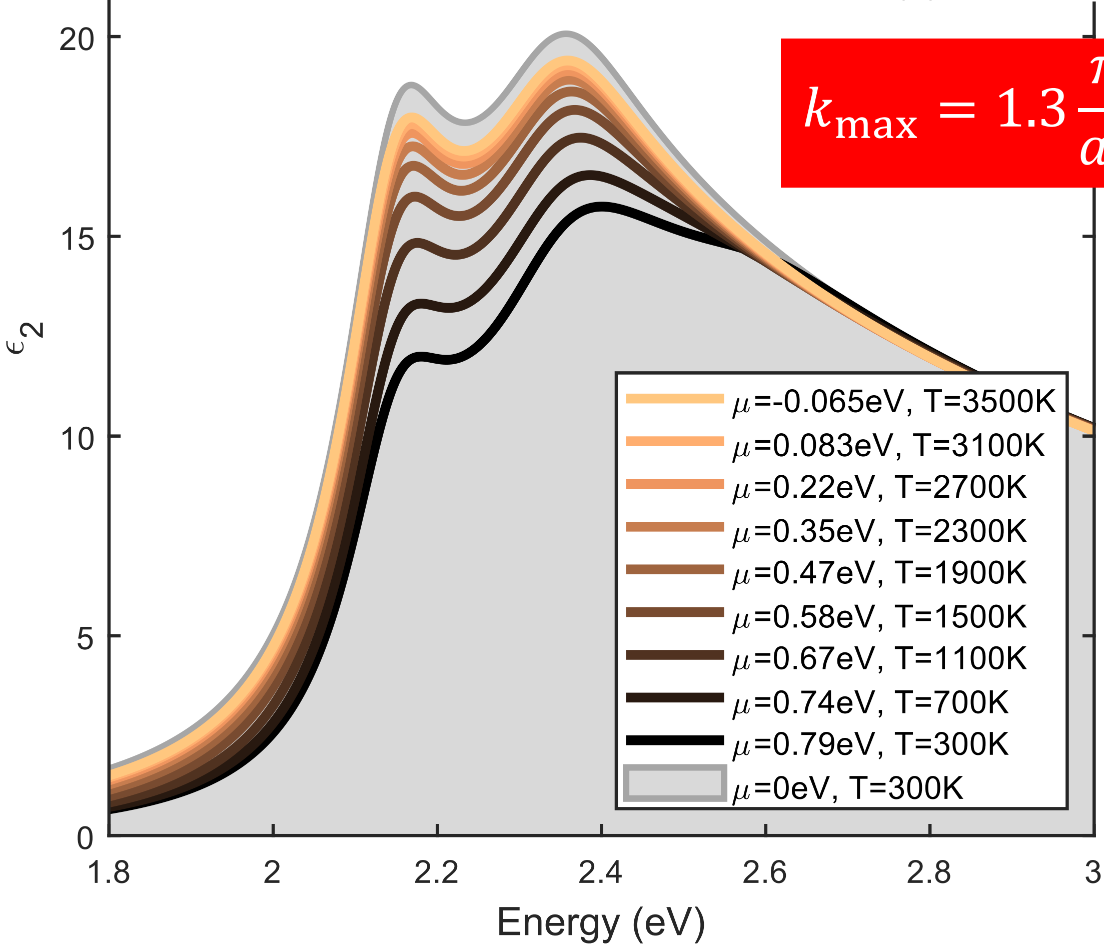

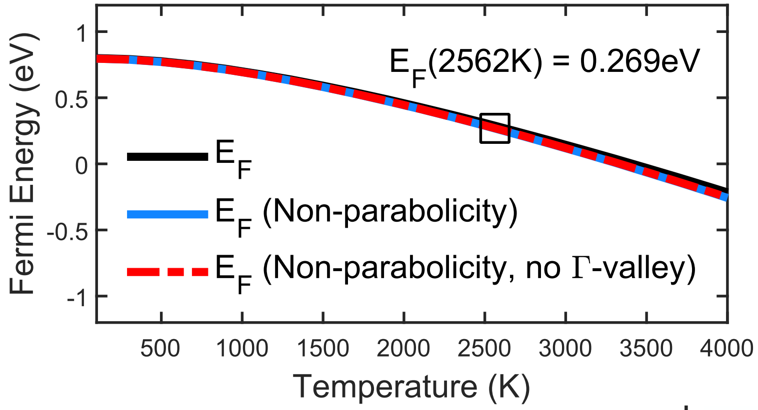

$$k_{\max} = 1.3\,\frac{\pi}{a_0}$$

Conclusion

- There is much interesting physics in the optical constants of α-tin and germanium-tin alloys.
- Kane's k.p band structure for InSb is the key.
  - Conduction band nonparabolicity.
  - **k-dependent dipole matrix elements (not yet included)**
- Chemical potential and Fermi-Dirac statistics
- Band filling (Pauli blocking) of transient optical absorption
- Excitonic enhancement of the interband transitions (3D, 2D)
- Screening of excitons at high carrier concentrations
- **How do we screen the absorption by 2D excitons?**
- **We are finishing the analysis for publication.**

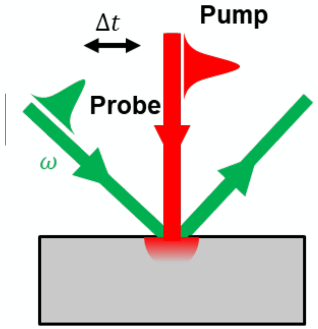

Email: zollner@nmsu.edu
Web: http://femto.nmsu.edu

Optical Spectroscopy of Materials for Mid-Wave Infrared Detector Applications

1. **Pressure dependence** of low-temperature photoluminescence of germanium-tin alloys (AFRL/RVSU);
   Today: Temperature dependence of photoluminescence of bulk **GaSb**.
2. **Thermal oxidation** of **bulk Ge**, thick Ge on Si, and Ge-Sn alloys on Si (NSF, Arizona State);
   Include AFM surface roughness and structural characterization with high-resolution XRD.
3. **Nonparabolicity** of conduction band of InSb (SFFP, AFOSR)
4. Direct gap **infrared absorption of α-tin** with nonparabolic bands (SFFP, AFOSR)
5. Low-temperature ellipsometry measurements (0.03 to 6.5 eV) with a **recirculating helium cooler** (ARO).
6. **Direct gap absorption of α-tin** on InSb and CdTe: experiment and theory (NSF, UCSB)
7. Excitonic enhancement of the absorption near the E_1 gaps of Ge (AFOSR)
8. Transient dielectric function of germanium from **femtosecond pump-probe ellipsometry** (AFOSR)

NM STATE BE BOLD. Shape the Future.

Email: zollner@nmsu.edu
Web: http://femto.nmsu.edu